Integrated analysis of environmental and genetic influences on cord blood DNA methylation in new-borns

Running title: Combination of genetic and environmental effects best explain DNA cordblood methylation in variably methylated regions

Darina Czamara[1], Gökçen Eraslan[2,3], Christian M. Page[4,5], Jari Lahti[6,7], Marius Lahti-Pulkkinen[6,8], Esa Hämäläinen[9], Eero Kajantie[10,11,12], Hannele Laivuori[13,14,15,16], Pia M Villa[13], Rebecca M. Reynolds[8], Wenche Nystad[17], Siri E Håberg[5], Stephanie J London[18], Kieran J O'Donnell[19,20], Elika Garg[19], Michael J Meaney[19,20,21], Sonja Entringer [22,23], Pathik D Wadhwa[23,24], Claudia Buss[22,23], Meaghan J Jones [25], David TS Lin[25] , Julie L MacIsaac[25], Michael S Kobor[25], Nastassja Koen[26,27], Heather J Zar[28], Karestan C Koenen[29], Shareefa Dalvie[26], Dan J Stein[26, 27], Ivan Kondofersky[2,30], Nikola S Müller[2], Fabian J Theis[2,30], Major Depressive Disorder Working Group of the Psychiatric Genomics Consortium†,, Katri Räikkönen[6] and Elisabeth B Binder*[1,31].

[1] Max-Planck-Institute of Psychiatry, Department of Translational Research in Psychiatry, Munich, Germany
[2] Institute of Computational Biology, Helmholtz-Zentrum München, German Research Center for Environmental Health, Neuherberg, Germany
[3] School of Life Sciences, Weihenstephan, Technische Universität München, Freising, Germany
[4] Oslo Centre for Biostatistics and Epidemiology, Research Support Unit, Oslo University Hospital, Oslo, Norway
[5] Center for Fertility and Health, Norwegian Institute of Public Health, Oslo, Norway
[6] Department of Psychology and Logopedics, Faculty of Medicine, University of Helsinki, Finland
[7] Helsinki Collegium for Advanced Studies, University of Helsinki, Finland
[8] British Heart Foundation Centre for Cardiovascular Science, Queen's Medical Research Institute, University of Edinburgh, UK
[9] HUSLAB and Department of Clinical Chemistry, Helsinki University, Helsinki, Finland
[10] Oulu University Hospital and University of Oulu, PEDEGO Research Unit, MRC Oulu, Finland

[11] Hospital for Children and Adolescents, University of Helsinki and Helsinki University Hospital, Finland
[12] National Institute for Health and Welfare, Helsinki, Finland
[13] Medical and Clinical Genetics and Obstetrics and Gynaecology University of Helsinki and Helsinki University Central Hospital, Finland
[14] Institute for Molecular Medicine Finland, Helsinki Institute of Life Science, University of Helsinki, Finland
[15] Faculty of Medicine and Life Sciences, University of Tampere, Tampere, Finland
[16] Department of Obstetrics and Gynecology, Tampere University Hospital, Tampere, Finland
[17] Department of Chronic Diseases and Ageing, Norwegian Institute of Public Health, Oslo, Norway
[18] Epidemiology Branch, National Institute of Environmental Health Sciences, National Institutes of Health, U.S. Department of Health and Human Services, Research Triangle Park, North Carolina, United States of America
[19] Ludmer Centre for Neuroinformatics and Mental Health, Douglas Mental Health University Institute, McGill University, Montreal, QC, Canada
[20] Sackler Program for Epigenetics and Psychobiology at McGill University, Montreal, QC, Canada
[21] Singapore Institute for Clinical Sciences, Singapore
[22] Charité – Universitätsmedizin Berlin, corporate member of Freie Universität Berlin, Humboldt-Universität zu Berlin, and Berlin Institute of Health (BIH), Institute of Medical Psychology, Berlin, Germany
[23] University of California, Irvine, Development, Health, and Disease Research Program, Orange, CA, USA
[24] Departments of Psychiatry and Human Behavior, Obstetrics and Gynecology, and Epidemiology, University of California, Irvine, School of Medicine, Irvine, CA, USA
[25] Centre for Molecular Medicine and Therapeutics, Department of Medical Genetics, University of British Columbia and the BC Children's Hospital Research Institute, Vancouver, BC, Canada
[26] Department of Psychiatry and Mental Health, University of Cape Town, South Africa
[27] South African Medical Research Council (SAMRC), Unit on Risk and Resilience in Mental Disorders, Cape Town, South Africa
[28] Department of Paediatrics & Child Health and SAMRC Unit on Child and Adolescent Health, University of Cape Town, South Africa
[29] Department of Epidemiology, Harvard T. H. Chan School of Public Health, Boston, MA, USA
[30] Department of Mathematics, Technische Universität München, Munich, Germany.
[31] Department of Psychiatry and Behavioral Sciences, Emory University School of Medicine, USA
† A full list of consortium members appears at the end of the paper.

Correspondence and requests for materials should be addressed to Elisabeth B. Binder (email: binder@psych.mpg.de).

Key words: cord blood, DNA methylation, variably methylated regions (VMRs), prenatal environment, epigenetics, methylation quantitative trait loci (meQTL), gene x environment interaction

Abstract

Epigenetic processes, including DNA methylation (DNAm), are among the mechanisms allowing integration of genetic and environmental factors to shape cellular function. While many studies have investigated either environmental or genetic contributions to DNAm, few have assessed their integrated effects. Here we examine the relative contributions of prenatal environmental factors and genotype on DNA methylation in neonatal blood at variably methylated regions (VMRs) in 4 independent cohorts (overall n=2,365).

We use Akaike's information criterion to test which factors best explain variability of methylation in the cohort-specific VMRs: several prenatal environmental factors (E), genotypes in cis (G), or their additive (G+E) or interaction (GxE) effects.

Genetic and environmental factors in combination best explain DNAm at the majority of VMRs. The CpGs best explained by either G, G+E or GxE are functionally distinct. The enrichment of genetic variants from GxE models in GWAS for complex disorders supports their importance for disease risk.

Introduction

Fetal or prenatal programming describes the process by which environmental events during pregnancy influence the development of the embryo with on-going implications for future health and disease. Several studies have shown that the *in utero* environment is associated with disease risk, including coronary heart disease [1,2], type 2 diabetes [3], childhood obesity [4,5] as well as psychiatric problems [6] and disorders [7-9].

Environmental effects on the epigenome, for example via DNA methylation, could lead to sustained changes in gene transcription and thus provide a molecular mechanism for the enduring influences of the early environment on later health [10]. Smoking during pregnancy influences widespread and highly reproducible differences in DNA methylation at birth [11]. Less dramatic effects have been reported for maternal body mass index (BMI) [12], pre-eclampsia and gestational diabetes [13,14]. Possible epigenetic changes as a consequence of prenatal stress are less well established [15]. Some of these early differences in DNA methylation persist, although attenuated, through childhood [11,16] and might be related to later symptoms and indicators of disease risk, including BMI during childhood [17,18] or substance use in adolescence [19]. These data emphasize the potential importance of the prenatal environment for the establishment of inter-individual variation in the methylome as a predictor or even mediator of disease risk trajectories.

In addition to the environment, the genome plays an important role in the regulation of DNA methylation. To this end, the impact of genetic variation, especially of single nucleotide polymorphisms (SNPs) on DNA methylation in different tissues, has resulted in the discovery of a large number of methylation quantitative trait loci (meQTLs, i.e., SNPs significantly associated with DNA methylation status [20]). These variants are primarily in cis, i.e., at most 1 million base pairs away from the DNA methylation site [20-22] and often co-occur with expression QTLs or

other regulatory QTLs [23-25]. The association of meQTLs with DNA methylation is relatively stable throughout the life course [21]. In addition, SNPs within meQTLs are strongly enriched for genetic variants associated with common disease in large genome-wide association studies (GWAS) such as BMI, inflammatory bowel disease, type 2 diabetes or major depressive disorder [21,23,24,26].

Environmental and genetic factors may act in an additive or multiplicative manner to shape the epigenome to modulate phenotype presentation and disease risk [27]. However, very few studies have so far investigated the joint effects of environment and genotype on DNA methylation, especially in a genome-wide context. Klengel et al. [28] , for instance, reported an interaction of the FK506 binding protein 5 gene (*FKBP5)* SNP genotype and childhood trauma on *FKBP5* methylation levels in peripheral blood cells, with trauma associated changes only observed in carriers of the rare allele. The most comprehensive study of integrated genetic and environmental contributions to DNA methylation so far was performed by Teh et al. [29]. This study examined variably methylated regions (VMRs), defined as regions of consecutive CpG-sites showing the highest variability across all methylation sites assessed on the Illumina Infinium HumanMethylation450 BeadChip array. In a study of 237 neonate methylomes derived from umbilical cord tissue, the authors explored the proportions of the influence of genotype vs. prenatal environmental factors such as maternal BMI, maternal glucose tolerance and maternal smoking on DNA methylation at VMRs. They found that 75% of the VMRs were best explained by the interaction between genotype and environmental factors (GxE) whereas 25% were best explained by SNP genotype and none by environmental factors alone. Collectively, these studies highlight the importance of investigating the combination of environmental and genetic contributions to DNA methylation and not only their individual contribution.

The main objective of the present study is to extend our knowledge of combined effects of prenatal environment and genetic factors on DNA methylation at VMRs. Specifically, this is addressed by: 1) assessing the stability of the best explanatory factors across different cohorts and whether this extends to all environmental factors, 2) dissecting differences between additive and interactive effects of gene and environment not explored in Teh et al., 3) testing whether VMRs influenced by genetic and/or environmental factors might have a different predicted impact on gene regulation and 4) evaluating the relevance of genetic variants that interact with the environment to shape the methylome for their contribution to genetic disease risk.

Our results show that across cohorts genetic variants in combination with prenatal environment are the best predictors of variance in DNA methylation. We observe functional differences of both the genetic variants and the methylation sites best explained by genetic or additive and interactive effects of genes and environment. Finally, the enrichment of genetic variants within additive as well as interactive models in GWAS for complex disorders supports the importance of these environmentally modified methylation quantitative trait loci for disease risk.

Results

Cohorts and analysis plan

We investigated the influence of the prenatal environment and genotype on VMRs in the DNA of 2,365 newborns within 4 different cohorts: Prediction and Prevention of Pre-eclampsia and Intrauterine Growth Restrictions (PREDO, cordblood) [30], the UCI cohort ([31-33], heel prick), the Drakenstein Child Health Study (DCHS, cordblood) [34,35] and the Norwegian Mother and Child Cohort Study (MoBa, cordblood [36]). A description of the workflow of this manuscript is given in Figure 1 and the details for each of the cohorts are given in Table 1.

Table 1: overview of investigated cohorts

cohort	PREDO I	PREDO II	DCHS I	DCHS II	UCI	MoBa
sample-size	817	146	107	151	121	1,023
methylation array	Illumina 450K	Illumina EPIC	Illumina 450K	Illumina EPIC	Illumina EPIC	Illumina 450K
Methylation data processing	Funnorm and Combat	Funnorm and Combat	SWAN and Combat	BMIQ and Combat	Funnorm and Combat	BMIQ and Combat
SNP genotyping	Illumina Human Omni Express Exome	Illumina Human Omni Express Exome	Illumina PsychArray	Illumina GSA	Illumina Human Omni Express	Illumina HumanExome Core
infant gender male	433 (53.0%)	75 (51.4%)	63 (58.8%)	83 (55.0%)	65 (53.7%)	478 (46.7%)
maternal age mean (sd)	33.28 (5.79)	32.25 (4.92)	26.27 (5.87)	27.42 (5.93)	28.47 (4.91)	29.92 (4.32)
partity mean (sd)	1.05 (1.02)	0.87 (1.03)	0.98 (1.12)	1.09 (1.07)	1.11 (1.15)	0.83 (0.88)
Caesarian section	169 (20.7%)	36 (24.7%)	19 (17.6%)	35 (23.2%)	37 (30.6%)	228 (22.3%)
pre-pregnancy BMI mean (sd)	27.42 (6.40)	25.37 (5.79)	not available	not available	27.90 (6.44)	24.05 (4.19)
maternal smoking yes	exclusion criterion	exclusion criterion	7.40 (10.52) [a)]	4.94 (9.43) [a)]	10 (8.2%)	148 (14.4%)
gestational diabetes yes	183 (22.4%)	19 (13.0%)	no cases available	no cases available	9 (7.4%)	15 (1.5%)
hypertension yes	275	31 (21.2%)	2 (.19%)	2 (1.3%)	7 (5.8%)	50 (4.9%)

	(33.7%)					
betamethasone treatment yes	35 (4.3%)	2 (1.5%)	not available	not available	no cases available	not available
anxiety score mean (sd)	33.93 (7.90) [b)]	34.43 (8.38) [b)]	5.70 (4.15) [c)]	5.32 (3.91) [c)]	1.67 (0.41) [d)]	4.79 (1.36) [e)]
depression score mean (sd)	11.34 (6.47) [f)]	11.53 (6.98) [f)]	17.64 (12.10) [g)]	12.52 (11.55) [g)]	0.68 (0.41) [h)]	5.24 (1.57) [e)]

[a)] based on ASSIST Tobacco Score
[b)] STAI sum scores
[c)] SRQ-20
[d)] STAI average scores
[e)] based on Hopkins Symptom Checklist
[f)] CESD sum scores
[g)] BDI-II
[h)] CESD average score

We analyzed 963 cord blood samples from the PREDO cohort with available genome-wide DNA methylation and genotype data. Of these samples, 817 had data on the Illumina 450k array (PREDO I) and 146 on the Illumina EPIC array (PREDO II). The main analyses are reported for PREDO I, and replication and extension of the results is shown for PREDO II as well as for three independent cohorts including 121 heel prick samples (UCI cohort, EPIC array) as well as 258 (DCHS, 450K and EPIC array) and 1,023 cord blood samples (MoBa, 450K array). We tested ten different prenatal environmental factors covering a broad spectrum of prenatal phenotypes (see Table 1) (referred to as E), as well as cis SNP genotype (referred to as G), i.e., SNPs located in at most 1MB distance to the specific CpG, additive effects of cis SNP genotype and prenatal environment (G+E) and cis SNP x environment interactions (GxE) for association with DNA methylation levels (see Figure 1). We then assessed for each VMR independently which model described the variance of DNAm best using Akaike's information criterion (AIC) [37]. In all models, we corrected for child's gender, ethnicity (using MDS-components), gestational age as well as estimated cell proportions to account for cellular heterogeneity.

Variably Methylated Regions

We first identified candidate VMRs, defined as regions of CpG-sites showing the highest variability across all methylation sites. In PREDO I, we identified 10,452 variable CpGs that clustered into 3,982 VMRs (see Supplementary Data 1). Most VMRs (n=2,683) include 2 CpGs. As detailed in Supplementay Note 1, the distribution of methylation levels of CpGs within these VMRs is unimodal, (see Supplementary Figure 1A), VMRs are enriched in specific functional regions of the genome, correlate with differences in gene expression, and overlap with sites associated with specific prenatal environmental factors.

To examine the factors that best explain the variance in methylation in these functionally relevant sites, we chose the CpG-site with the highest MAD-score as representative of the VMR. These CpGs are named tagCpGs. The correlation between methylation levels of tagCpG and average methylation of the respective VMR was high (mean r=0.85, sd r=0.08), suggesting that the tag CpGs are valid representatives of their VMRs. Furthermore, tagCpGs are mainly uncorrelated with each other (mean r=0.03, sd=0.12).

Which models explain methylation of tagCpGs best?

We next compared the fit of four models for each of the 3,982 tagCpGs (see Figure 1): best SNP (G model), best environment (E model), SNP + environment (G+E model) and SNP x environment (GxE model). Association results for each model are listed in Supplementary Data 2-5. For each tagCpG, the model with the lowest AIC was chosen as the best model (see Methods section). In total, 40.6% of tagCpGs were best explained by GxE (n=1,616), followed by G (30%, n=1, 194) and G+E (29%, n=1,171) (Figure 2A). E explained most variance in one tagCpG. All tag CpGs and the respective SNPs and environments from the best model are listed in Supplementary Data 6-8 and Supplementary Table 1.

With regard to environmental factors, 27.0% of tagCpGs best explained by the G+E model were associated with environmental factors related with stress or, in particular, glucocorticoids (i.e., maternal betamethasone treatment), 40.8% with general maternal factors (mostly maternal age) and 32.20 % with factors related to metabolism (pre-pregnancy BMI, hypertension, gestational diabetes). For best model GxE tagCpGs, the proportions of environmental factors were similar with 22.2%, 44.1% and 33.7%, respectively (see Figure 2B).

We next looked into the delta AIC, i.e., the difference between the AIC of the best model to the AIC of the next best model (see Supplementary Note 2). GxE models appear to be winning by a significantly larger AIC margin over the next best model, when compared to the other types of winning models (see Figure 2C).

DeepSEA prediction of SNP function

We were next interested in understanding the functionality of both the VMRs as well as the associated SNPs in the G, GxE and G+E models. For this we restricted the analyses only to potentially functional relevant SNPs using DeepSEA [38] and not all linkage disequilibrium (LD)-pruned SNPs as described above. DeepSEA, a deep neural network pretrained with DNase-seq and ChIP-seq data from the ENCODE [39] project, predicts the presence of histone marks, DNase hypersensitive regions (DHS) or TF binding for a given 1kb sequence. The likelihood that a specific genetic variant influences regulatory chromatin features is estimated by comparing predicted probabilities of two sequences where the bases at the central position are the reference and alternative alleles of a given variant. We reran the four models now restricting the cis-SNPs to those 36,241 predicted DeepSEA variants that were available in our imputed, quality-controlled genotype dataset.

Top results for models including G, GxE and G+E are depicted in Supplementary Data 9-12. Results were comparable to what we observed before: 1,195 (30.09%) of tagCpGs presented with best model G, 1,193 CpGs (30.04%) with best model G+E, 1,510 CpGs (38.02 %) with best model GxE and 74 CpGs (1.86%) with best model E (Figure 3A) and also showed similar differences in delta-AIC and proportions of E categories (see Supplementary Note 3). Only 10 tagCpGs did not present with any DeepSEA variant within 1MB distance in cis and were therefore not further considered. All respective CpG-environment-DeepSea SNP-combinations are depicted in Supplementary Data13-16.

The distribution of best models was not influenced by the degree of variability of DNA methylation, but was comparable across the whole range of DNA methylation variation (see Supplementary Note 4 and Supplementary Figure 2). A slight enrichment for G+E models was observed in longer VMRs with at least 3 CpGs ($p=9.00 \times 10^{-06}$, OR=1.39, Fisher-test, see Supplementary Figure 3).

In conclusion, also when we focus on potentially functionally relevant SNPs, it is the combination of genotype and environment which best explains VMRs.

We observed that, as expected, different types of exposures or maternal factors have different relative impact on DNA methylation (see Supplementary Note 5). However, even for those exposures with the highest fraction of VMRs best explained by E alone, combined models of G+E and GxE remain the best models in even higher fractions of VMRs (see Supplementary Figure 4B).

Functional annotation of different best models

Focusing on combinations between tagCpGs, environmental factors and DeepSEA variants, we found functional differences for both the SNPs as well as the tagCpGs (see Supplementary Note 6) within the different models. Overall, 895 DeepSEA variants were uniquely involved in best G models, 905 were uniquely in best G+E models and 1,162 uniquely in best GxE models. As a DeepSEA variant can be in multiple 1 MB-cis windows around the tagCpGs, several DeepSEA variants were involved in multiple best models: 138 DeepSEA variants overlapped between G and GxE, 118 between G and G+E and 147 between GxE and G+E VMRs. We observed no significant differences with regard to gene-centric location for DeepSEA variants involved only in G models, only in G+E models or in multiple models. However, DeepSEA variants involved only in GxE models were significantly depleted for promoter locations ($p=3.92 \times 10^{-02}$, OR=0.79, Fisher-test, see Supplementary Figure 5A).

Although no significant differences were present, DeepSEA SNPs involved in the G and G+E model were located in closer proximity to the specific CpG (model G: mean absolute distance=256.8 kb, sd=291.2 kb, model G+E: mean absolute distance =244.8 kb, sd=284.0 kb, Supplementary Figure 5B) whereas DeepSEA SNPs involved in GxE models (mean absolute distance =352.6 kb, sd=305.3 kb) showed broader peaks around the CpGs.

With regards to histone marks, DeepSEA variants in general were enriched across multiple histone marks indicative of active transcriptional regulation (Figure 4C). DeepSEA variants involved in best model G+E showed further enrichment for strong transcription ($p=7.19 \times 10^{-03}$, OR=1.34, Fisher-test) as well as depletion for quiescent loci ($p=7.17 \times 10^{-03}$, OR=0.78, Fisher-test). In contrast, GxE DeepSEA variants were significantly enriched in these regions ($p=2.62 \times 10^{-02}$, OR=1.22, Fisher-test, Figure 4D).

Taken together, these analyses indicate that both the genetic variants and the VMRs in the different best models (G, GxE and G+E) preferentially annotate to functionally distinct genomics regions.

Replication of best models in independent cohorts

To assess whether the relative distribution of the best models for VMRs and DeepSEA variants was stable across different samples, we assessed the relative distribution of these models in 3 additional samples (DCHS I and DCHS II, UCI and PREDOII) with VMR data both from the Illumina 450K as well as the IlluminaHumanEPIC arrays. Information on these cohorts is summarized in Table 1 and the number of VMRs, the distribution of VMR methylation levels, VMR length and specific SNP information are given in Supplementary Note 7 and Supplementary Figure 6.

While major maternal factors overlapped among the cohorts - such as maternal age, delivery method, parity and depression during pregnancy - there were also differences, as the non-PREDO cohorts did not include betamethasone treatment but additionally included maternal smoking (see Table 1). Despites these differences and differences in the total number of VMRs, the overall pattern remained stable: in all 4 analyses, DCHS I, DCHS II, UCI and PREDO II, we replicated that E alone models almost never explained most of the variances, while G alone models explained the most variance in up to 15% of the VMRs; G+E in up to 32%; and GxE models in up to 60% (see Figure 5 and Table 2).

Table 2: VMRs and best models across cohorts

cohort	PREDO I	PREDO II	DCHS I	DCHS II	UCI
sample-size	817	146	107	151	121
methylation array	Illumina 450K	Illumina EPIC	Illumina 450K	Illumina EPIC	Illumina EPIC

# VMRs	3,972	8,547	6,072	10,005	9,525
proportion: best model E	2.0%	<1%	<1%	<1%	4.1%
best model G	30.0%	15.0%	15.8%	11.5%	12.8%
best model G+E	30.0%	29.0%	29.8%	32.1%	24.1%
best model GxE	38.0%	56.0%	54.3%	56.3%	59.0%

The importance of including G for a best model fit could also be observed for maternal smoking, described as one of the most highly replicated factors shaping the newborns' methylome [11] and present in the replication but not the discovery cohort PREDO I. These analyses are detailed in Supplementary Note 8.

We were also able to replicate our finding showing that GxE VMRs were enriched for OpenSea positions with a trend on the 450K array (DCHS I, OR=1.11, $p= 5.03x10^{-02}$, Fisher-test) and significantly for the EPIC array data (PREDOII: $p=2.96x10^{-06}$, OR=1.29, UCI: $p= 3.79x10^{-02}$, OR=1.09, DCHSII: $p=2.91x10^{-04}$, OR=1.16, Fisher-tests). For all additional cohorts, the delta AIC for best model GxE to the next best model was also significantly higher as compared to CpGs with G, E or G+E as the best model.

Overall, 387 tag CpGs overlapped between PREDO I, PREDO II, DCHS I and DCHS II (see Supplementary Figure 7), which allowed us to test the consistency of the best models for specific VMRs across the different cohorts. Over 70% of the overlapping tagCPGs showed consistent best models in at least 3 cohorts (see Figure 6) with GxE being the most consistent model (for over 60% of consistent models, see Supplementary Figure 8). Focusing only on EPIC data (PREDO II, DCHSII and UCI), we identified more, namely 2,091, tag CpGs that overlap across the three cohorts and here 86% show a consistent best model in at least two of the three cohorts, despite differences in study design, prenatal phenotypes and ethnicity.

Thus, the additional cohorts not only showed a consistent replication of the proportion of the models best explaining variance of VMRs but also consistency of the best model for specific

VMRs. Within this context, we observed the GxE models were the most consistent models across the cohorts (, see Supplementary Figure 8), with 85% of the CpGs with consistent models across 5 cohorts having GxE as the best model. Furthermore, we could validate specific GxE combinations between PREDO I and MoBa as shown as in the Supplementary Note 9.

Disease relevance

Finally, we tested whether functional DeepSEA SNPs involved in only G, only GxE and only G+E models in PREDO I for their enrichment in GWAS hits. We used all functional SNPs and their LD proxies (defined as r^2 of at least 0.8 in the PREDO cohort and in maximal distance of 1MB to the target SNP) and performed enrichment analysis with the overlap of nominal significant GWAS hits. We selected for a broad spectrum of GWAS, including GWAS for complex disorders for which differences in prenatal environment are established as risk factors, but also including GWAS on other complex diseases. For psychiatric disorders, we used summary statistics of the Psychiatric Genomics Consortium (PGC) including association studies for autism [40], attention-deficit-hyperactivity disorder [41], bipolar disorder [42], major depressive disorder [43], schizophrenia [44] and the cross-disorder associations including all five of these disorders [45]. Additionally, we included GWAS of inflammatory bowel disease [46], type 2 diabetes [47] and for BMI [48]. Nominal significant GWAS findings were enriched for DeepSEA variants and their LD proxies per se across psychiatric as well as non-psychiatric diseases (Figure 7A). However, G, GxE and G+E DeepSEA variants showed a differential enrichment pattern above all DeepSEA variants (Figure 7B), with strongest enrichments of GxE DeepSEA variants in GWAS of autism spectrum disorder ($p<2.20 \times 10^{-16}$,OR=2.07 above DeepSEA, Fisher-test), attention-deficit-hyperactivity disorder ($p<2.20 \times 10^{-16}$, OR=1.71, Fisher-test) and inflammatory

bowel disease ($p<2.20 \times 10^{-16}$, OR=1.71, Fisher-test) and G+E DeepSEA variants in GWAS for attention-deficit-hyperactivity disorder ($p=9.54 \times 10^{-36}$, OR=1.23, Fisher-test) and inflammatory bowel disease ($p=1.85 \times 10^{-52}$, OR=1.30, Fisher-test). While SNPs with strong main meQTL effects such as those within G and G+E models have been reported to be enriched in GWAS for common disease, we now also show this for SNPs within GxE models that often have non-significant main G effects.

Discussion

We evaluated the effects of prenatal environmental factors and genotype on DNA methylation at VMRs identified in neonatal blood samples. We found that most variable methylation sites were best explained by either genotype and prenatal environment interactions (GxE) or additive effects (G+E) of these factors, followed by main genotype effects. This pattern was replicated in independent cohorts and underscores the need to consider genotype in the study of environmental effects on DNA methylation.

In fact, VMRs best explained by G, G+E or GxE and their associated functional genetic variants were located in distinct genomic regions, suggesting that different combinatorial effects of G and E may impact VMRs with distinct downstream regulatory effects and thus possibly context-dependent impact on cellular function. We also observed that functional variants with best models G, G+E or GxE, all showed significant enrichment within GWAS signals for complex disorders beyond the enrichment of the functional variants themselves. While this was expected for G and G+E models based on results from previous studies [21,23,24,26], it was surprising for GxE SNPs, as these often do not have highly significant main genetic effects. Their specific enrichment in GWAS for common disorders supports the importance of these genetic variants

that moderate environmental impact both at the level of DNA methylation but also, potentially, for disease risk.

The fact that GxE and G+E best explained the majority of VMRs (see Figure 5) and that GxE models were selected by a larger margin than the other models (see Figure 2C) was consistently found across all tested cohorts. These findings are in line with a previous report by Teh et al. [29] who performed a similar analysis based on AIC in umbilical cord tissue. Differences to the findings by Teh et al. are discussed in the Supplemental Discussion. Using data from 4 different cohorts, we not only saw comparable proportions of VMRs best explained by the different models, but also saw in the VMRs common across cohorts that specific VMRs had consistent best models (see Figure 6). This is in line with the fact that VMRs best explained by G, GxE or G+E show functional differences and may differentially impact gene regulation.

In addition to consistent findings using AIC-based approaches, we also observed some indication for validation of individual GxE and G+E combinations on selected VMRs using p-value based criteria, with a small number of specific G+E and GxE effects on VMRs replicating between the PREDO I and the MoBa cohort. The low number of specific replications could be due to lack of overall power as well as larger differences in prenatal factors between these two cohorts (see Table 1). As shown in Supplementary Figure 4B, which specific G and E combinations best explain VMRs is also dependent on the specific prenatal factors. Larger and more homogenous cohorts regarding exposures will be needed for such analyses to be more conclusive.

While E alone was rarely the best model, it should be pointed out that main environmental effects on DNA methylation were observed (see Supplementary Data 3), and consistent with previous large meta-analyses such as in the case of maternal smoking (see Supplementary Notes 7). Within the MoBa cohort, the cohort with the largest proportion of maternal smoking, 10% of

all tagCpGs were best explained by maternal smoking alone. However, in all other cohorts, where smoking was less prevalent, the inclusion of genotypic effects in addition to maternal smoking explained more of the variance. This supports that while main E effects on the newborn methylome are present, genotype is an important factor that, in combination with E, may explain even more of the variance in DNA methylation.

VMRs best explained by either E, G, G+E or GxE and their associated functional SNPs were enriched for distinct genomics locations and chromatin states (see Figure 4), suggesting that VMRs moderated by different combinations of G and E may in fact have distinct functional roles in gene regulation. Overall, VMRs best explained by GxE were consistently enriched for regions annotated to the OpenSea regions with lower CpG density and located farthest from CpG Islands [49]. Open Sea regions have been reported to be enriched for environmentally-associated CpGs with for example exposure to childhood trauma [50] and may harbor more long-range enhancers. In addition to their position relative to CpG islands and their CpG content, G, GxE and G+E VMRs and their associated functional SNPs also showed distinct enrichments for chromatin marks. Compared to 450K VMRs in general, VMRs with GxE as the best models were relatively depleted in regions surrounding the TSS, while VMRs with G+E were relatively enriched in these regions (see Figure 4), suggesting that GxE VMRs are located at more distance from the TSS than G+E VMRs. To better map the potential functional variants in these models and to compare methylation-associated SNPs from a regulatory perspective, we used DeepSEA [38], a machine learning algorithm that predicts SNP functionality from the sequence context based on sequencing data for different regulatory elements in different cell lines using ENCODE data [39]. We identified the SNPs with putatively functional consequences on regulatory marks by DeepSEA and compared putative regulatory effects of G, G+E and GxE hits. Relative to the

413 imputed non-DeepSEA SNPs contained in our dataset, these predicted functional DeepSEA
414 SNPs were enriched for TSS and enhancer regions and depleted for quiescent regions, supporting
415 their relevance in regulatory processes (see Figure 4). Compared to DeepSEA SNPs overall,
416 DeepSEA SNPs within the 3 different best models also showed distinct enrichment or depletion
417 patterns. Similar to GxE VMRs, likely functional GxE SNPs also showed a relative depletion in
418 TSS regions while G+E SNPs showed enrichment in genic enhancers. Overall, both the VMRs
419 as well as the associated functional SNPs appear to be in distinct regulatory regions, depending
420 on their best model. In addition, GxE functional SNP and tagCpGs were located farther apart
421 than SNP/tagCpG pairs within G or G+E models (see Supplementary Figure 5B), supporting a
422 more long-range type of regulation in GxE interactions on molecular traits as compared to all
423 genes; a similar relationship has been reported previously for GxE with regard to gene
424 expression in *C. elegans* [51,52].
425 SNPs associated with differences in gene expression but also DNA methylation have consistently
426 been shown to be enriched among SNPs associated with common disorders in GWAS [21,24,26,53].
427 The functional genetic variants that were within G, GxE or G+E models predicting variable
428 DNA methylation were even enriched in GWAS association results (beyond the baseline
429 enrichment of DeepSea SNPs per se). The fact that such enrichment was observed for not only G
430 and G+E SNPs, with strong main genetic effects, but also for GxE SNPs, with smaller to
431 sometimes no main genetic effect on DNA methylation underscores the importance of also
432 including SNPs within GxE models in the functional annotation of GWAS. A detailed catalogue
433 of meQTLs that are responsive to environmental factors could support a better
434 pathophysiological understanding of diseases for which risk is shaped by a combination of
435 environment and genetic factors.

436 Finally, we want to note the limitations of this study. First, we restricted our analyses to specific
437 DNA methylation array contents that are inherently biased as compared to genome-wide bisulfite
438 sequencing, for example. In addition, we restricted our analysis to VMRs, which also limits the
439 generalizability of the findings, but also has advantages. Ong and Holbrooke [54] showed that this
440 approach increases statistical power. Furthermore, VMRs are enriched for enhancers and
441 transcription factor binding sites, overlap with GWAS hits [55] and are associated with gene-
442 expression of nearby genes at these sites [56]. VMRs in this study presented with intermediate
443 methylation levels which have been shown to be enriched in regions of regulatory function, like
444 enhancers, exons and DNase I hypersensitivity sites [57]. Hence, the effects of genotypes on
445 DNA methylation levels in VMRs might be higher as compared to less variable CpG-sites. In
446 addition, genotypes are measured with much less error as compared to environmental factors
447 which may also reduce the overall explained variance in large cohorts.
448 Second, it has been reported that different cell types display different patterns of DNA
449 methylation [55]. Therefore, the most variable CpG-sites may also include those that reflect
450 differences in cord blood cell type proportions. To address this issue, all analyses were corrected
451 for estimated cell proportions to the best of our current availability, so that differences in cell
452 type proportion likely do not account for all of the observed effects. However, only replication
453 in specific cell types will be able to truly assess the proportion of VMRs influenced by this.
454 Third, we used the AIC as main criterion for model fit [37] which is equivalent to a penalized
455 likelihood-function. There are a variety of other model selection criteria [58] and choosing between
456 these is an ongoing debate which also depends on the underlying research question. We decided
457 to use the AIC as one of our main aims was to compare our results with the study of Teh et al. [29]

458 in which this criterion was applied and as this method maybe more powerful for detecting GxE
459 than for example model selection criteria based on lowest p-values.
460 Fourth, all reported interactions are statistical interactions and limited to a *cis* window around the
461 CpG-site. Further experiments are required to assess whether these would also reflect
462 biological/mechanistic interactions. Much larger cohorts will be needed to assess potential *trans*
463 effects. Additional inclusion of further covariates such as maternal smoking or maternal age may
464 further modify the effects of specific Es but is beyond the scope of this manuscript.
465 Fifth, as summarized in Table 1, results presented are based on cohorts which differ in ethnicity,
466 assessed phenotypes, methylation and SNP arrays, processing pipelines and sample sizes. While
467 all these factors may contribute to differences in the proportions of models across the cohorts, it
468 also suggests that our findings are quite robust to these methodological issues.
469 Finally, our analyses are restricted to DNA methylation in neonatal blood and to pregnancy
470 environments. Whether similar conclusions can be drawn for methylation levels assessed at a
471 later developmental stage needs to be investigated.
472 We tested whether genotype, a combination of different prenatal environmental factors and the
473 additive or the multiplicative interactive effects of both mainly influence VMRs in the newborn's
474 epigenome. Our results show that G in combination with E are the best predictors of variance in
475 DNA methylation. This highlights the importance of including both individual genetic
476 differences as well as environmental phenotypes into epigenetic studies and also the importance
477 of improving our ability to identify environmental associations. Our data also support the disease
478 relevance of variants predicting DNA methylation together with the environment beyond main
479 meQTL effects, and the view that there are functional differences of additive and interactive
480 effects of genes and environment on DNA methylation. Improved understanding of these

functional differences may also yield novel insights into pathophysiological mechanisms of common non-communicable diseases, as risk for all of these disorders is driven by both genetic and environmental factors.

Methods

The PREDO cohort

The Prediction and Prevention of Preeclampsia and Intrauterine Growth Restriction (PREDO) Study is a longitudinal multicenter pregnancy cohort study of Finnish women and their singleton children born alive between 2006-2010 [30]. We recruited 1,079 pregnant women, of whom 969 had one or more and 110 had none of the known clinical risk factors for preeclampsia and intrauterine growth restriction. The recruitment took place when these women attended the first ultrasound screening at 12+0-13+6 weeks+days of gestation in one of the ten hospital maternity clinics participating in the study. The cohort profile [30] contains details of the study design and inclusion criteria.

Ethics

The study protocol was approved by the Ethical Committees of the Helsinki and Uusimaa Hospital District and by the participating hospitals. A written informed consent was obtained from all women.

Maternal characteristics

We tested 10 different maternal environments:

Depressive symptoms

Starting from 12+0-13+6 gestational weeks+days pregnant women filled in the 20 item Center for Epidemiological Studies Depression Scale (CES-D) [59] for depressive symptoms in the past 7 days. They filled in the CES-D scale biweekly until 38+0-39+6 weeks+days of gestation or delivery. We used the mean-value across all the CES-D measurements.

Symptoms of anxiety

At 12+0-13+6 weeks+days of gestation, women filled in the 20 item Spielberger's State Trait Anxiety Inventory (STAI) [60] for anxiety symptoms in the past 7 days. They filled in the STAI scale biweekly until 38+0-39+6 weeks+days of gestation or delivery. We used the mean-value across all these measurements.

Betamethasone

Antenatal betamethasone treatment (yes/no) was derived from the hospital records and the Finnish Medical Birth Register (MBR).

Delivery method

Mode of delivery (vaginal delivery vs. caesarean section) was derived from patient records and MBR.

Parity

Parity (number of previous pregnancies leading to childbirth) at the start of present pregnancy was derived from the hospital records and the MBR.

Maternal age

Maternal age at delivery (years) was derived from the hospital records and the MBR.

Pre-pregnancy BMI

524 Maternal pre-pregnancy BMI (kg/m^2), calculated from measurements weight and height verified
525 at the first antenatal clinic visit at 8+4 (SD 1+3) gestational week was derived from the hospital
526 records and the MBR.
527 *Hypertension*
528 Hypertension was defined as any hypertensive disorder including gestational hypertension,
529 chronic hypertension and preeclampsia against normotension. Gestational hypertension was
530 defined as systolic/diastolic blood pressure ≥140/90 mm Hg on ≥ 2 occasions at least 4 h apart in
531 a woman who was normotensive before 20^{th} week of gestation. Preeclampsia was defined as
532 systolic/diastolic blood pressure ≥140/90 mm Hg on ≥2 occasions at least 4 h apart after 20^{th}
533 week of gestation and proteinuria ≥300 mg/24 h. Chronic hypertension was defined as
534 systolic/diastolic blood pressure ≥140/90 mm Hg on ≥2 occasions at least 4 h apart before 20^{th}
535 gestational week or medication for hypertension before 20 weeks of gestation.
536 *Gestational diabetes and oral glucose tolerance test (OGTT)*
537 Gestational diabetes was defined as fasting, 1h or 2h plasma glucose during a 75g oral glucose
538 tolerance test ≥5.1, ≥10.0 and/or ≥8.5 mmol/L, respectively, that emerged or was first identified
539 during pregnancy. We took the area under the curve from the three measurements as a single
540 measure for the OGTT itself.
541 *Genotyping and Imputation*
542 Genotyping was performed on Illumina Human Omni Express Exome Arrays containing 964,193
543 SNPs. Only markers with a call rate of at least 98%, a minor allele frequency of at least 1% and
544 a p-value for deviation from Hardy-Weinberg-Equilibrium > 1.0×10^{-06} were kept in the
545 analysis. After QC, 587,290 SNPs were available.

In total, 996 cord blood samples were genotyped. Samples with a call rate below 98% (n=11) were removed.

Any pair of samples with IBD estimates > 0.125 was checked for relatedness. As we corrected for admixture in our analyses using MDS-components (see Supplemental Figure 10), these samples were kept except for one pair which could not be resolved. From this pair we excluded one sample from further analysis. Individuals showing discrepancies between phenotypic and genotypic sex (n=1) were removed. We also checked for heterozygosity outliers but found none. 983 participants were available in the final dataset.

Before imputation, AT and CG SNPs were removed. Imputation was performed using shapeit2 (https://mathgen.stats.ox.ac.uk./genetics_software/shapeit/shapeit.html) and impute2 (https://mathgen.stats.ox.ac.uk/impute/impute_v2.html). Chromosomal and base pair positions were updated to the 1000 Genomes Phase 3 reference set, allele strands were flipped where necessary.

After imputation, we reran quality control, filtering out SNPs with an info score < 0.8, a minor allele frequency below 1% and a deviation from HWE with a p-value < 1.0×10^{-06}.

This resulted in a dataset of 9,402,991 SNPs. After conversion into best guessed genotypes using a probability threshold of 90%, we performed another round of QC (using SNP-call rate of least 98%, a MAF of at least 1% and a p-value threshold for HWE of 1.0×10^{-06}), after which 7,314,737 SNPs remained for the analysis.

For the evaluation of which model best explained the methylation sites, we pruned the dataset using a threshold of r^2 of 0.2 and a window-size of 50 SNPs with an overlap of 5 SNPs. The final, pruned dataset contained 788,156 SNPs. 36,241 of these variants were DeepSea variants (see Methods below).

Methylation

Cord blood samples were run on Illumina 450k Methylation arrays. The quality control pipeline was set up using the R-package *minfi* [61] (https://www.r-project.org). Three samples were excluded as they were outliers in the median intensities. Furthermore, 20 samples showed discordance between phenotypic sex and estimated sex and were excluded. Nine samples were contaminated with maternal DNA according to the method suggested by Morin et al. [62] and were also removed.

Methylation beta-values were normalized using the *funnorm* function [63]. After normalization, two batches, i.e., slide and well, were significantly associated and were removed iteratively using the *Combat* function [64] in the *sva* package [65].

We excluded any probes on chromosome X or Y, probes containing SNPs and cross-hybridizing probes according to Chen et al. [53] and Price et al [66]. Furthermore, any CpGs with a detection p-value > 0.01 in at least 25% of the samples were excluded.

The final dataset contained 428,619 CpGs and 822 participants. For 817 of these, also genotypes were available.

An additional 161 cord blood samples were run on Illumina EPIC Methylation arrays.

Three samples were excluded as they were outliers in the median intensities. Three samples showed discordance between phenotypic sex and estimated sex and were excluded. Three samples were contaminated with maternal DNA and were also removed [62].

Methylation beta-values were normalized using the *funnorm* function [63] in the R–package *minfi* [61]. Three samples showed density artefacts after normalization and were removed from further analysis. We excluded any probes on chromosome X or Y, probes containing SNPs and cross-hybridizing probes according to Chen et al. [53], Price et al. [66] and McCartney et al. [67].

592 Furthermore, any CpGs with a detection p-value > 0.01 in at least 25% of the samples were
593 excluded. The final dataset contains 812,987 CpGs and 149 samples. After normalization no
594 significant batches were identified. For 146 of these samples, genotypic data was also available.
595 Cord blood cell counts were estimated for seven cell types (nucleated red blood cells,
596 granulocytes, monocytes, natural killer cells, B cells, CD4(+)T cells, and CD8(+)T cells) using
597 the method of Bakulski et al. [68] which is incorporated in the R-package *minfi* [61].
598 *Identification of VMRs (variable methylated regions)*
599 The VMR approach was described by Ong and Holbrook [54]. We chose all 42,862 CpGs with a
600 MAD score greater than the 90th percentile. For each CpG-site, the MAD (median absolute
601 deviation) is defined as the median of the absolute deviations from each individual's methylation
602 beta-value at this CpG-site to the CpG's median. A candidate VMR region was defined as at
603 least two spatially contiguous probes which were at most 1kb apart of each other. This resulted
604 in 3,982 VMRs in the 450K samples and in 8,547 VMRs in the EPIC sample. The CpG with the
605 highest MAD scores was chosen as representative of the whole VMR in the statistical analysis.
606
607 *Drakenstein cohort*
608 Details on this cohort and the assessed phenotypes can be found in [34,35]. The birth cohort design
609 recruits pregnant women attending one of two primary health care clinics in the Drakenstein sub-
610 district of the Cape Winelands, Western Cape, South Africa – Mbekweni (serving a black
611 African population) and TC Newman (serving a mixed ancestry population). Consenting mothers
612 were enrolled during pregnancy, and mother–child dyads are followed longitudinally until
613 children reach at least 5 years of age. Mothers are asked to request that the father of the index

614 pregnancy attend a single antenatal study visit where possible. Follow-up visits for mother–child
615 dyads take place at the two primary health care clinics and at Paarl Hospital.
616 Pregnant women were eligible to participate if they were 18 years or older, were accessing one
617 of the two primary health care clinics for antenatal care, had no intention to move out of the
618 district within the following year, and provided signed written informed consent. Participants
619 were enrolled between 20 and 28 weeks' gestation, upon presenting for antenatal care visit. In
620 addition, consenting fathers of the index pregnancy when available were enrolled in the study
621 and attended a single antenatal study visit.
622 *Ethics*
623 The study was approved by the Faculty of Health Sciences, Human Research Ethics Committee,
624 University of Cape Town (401/2009), by Stellenbosch University (N12/02/0002), and by the
625 Western Cape Provincial Health Research committee (2011RP45). All participants provided
626 written informed consent.
627 *Maternal characteristics*
628 After providing consent, participants were asked to complete a battery of self-report and
629 clinician-administered measures at a number of antenatal and postnatal study visits. All assessed
630 phenotypes are described in detail in [34]. Here, we give a short outline on the phenotypes which
631 were used in our analysis. Maternal parity was obtained from the antenatal record; maternal age
632 was from the date of birth as recorded on the mothers' national identity document. The mode of
633 delivery was ascertained by direct observation of the birth by a member of the study team as all
634 births occurred at Paarl hospital. The SRQ-20 [69] is a WHO-endorsed measure of psychological
635 distress consisting of 20 items which assess non-psychotic symptoms, including symptoms of
636 depressive and anxiety disorders. Each item is scored according to whether the participant

responds in the affirmative (scored as 1) or negative (scored as 0) to the presence of a symptom. Individual items are summed to generate a total score. The Beck Depression Inventory (BDI-II) is a widely-used and reliable measure of depressive symptoms [70]. The BDI-II comprises 21 items, each of which assesses the severity of a symptom of major depression. Each item is assessed on a severity scale ranging from 0 (absence of symptoms) to 3 (severe, often with functional impairment). A total score is then obtained by summing individual item responses, with a higher score indicative of more severe depressive symptoms.

Smoking was assessed using The Alcohol, Smoking and Substance Involvement Screening Test (ASSIST) [71], a tool that was developed by the WHO to detect and manage substance use among people attending primary health care services. The tool assesses substance use and substance-related risk across 10 categories (tobacco, alcohol, cannabis, cocaine, amphetamine-type stimulants, inhalants, sedatives/sleeping pills, hallucinogens, opioids, and other substances), as well as enquiring about a history of intravenous drug use. Total scores are obtained for each substance by summing individual item responses, with a higher score indicative of greater risk for substance-related health problems.

Hypertension was assessed by blood pressure measured antenatally.

Genotyping and Imputation

Genotyping in DCHS was performed using the Illumina PsychArray for those samples with 450k data, or the Illumina GSA for those samples with EPIC DNA methylation data (Illumina, San Diego, USA). For both array types, QC and imputation was the same; first, raw data was imported into Genome Studio and exported into R for QC. SNPs were filtered out if they had a tenth percentile GC score below 0.2 or an average GC score below 0.1, for a total of 140 SNPs

removed. Phasing was performed using shapeit, and imputation was performed using impute2 with 1000 Genomes Phase 1 reference data. After imputation, we used qctool to filter out SNPs with an info score <0.8 or out of Hardy-Weinberg equilibrium. All SNPs with MAF <1% were removed.

As after imputation, only 5,286 DeepSEA variants were available for those samples genotyped on the PsychArray and only 4,049 for those samples genotyped on the GSAchip , we performed LD-pruning based on a threshold of r^2 of 0.2 and a window-size of 50 SNPs with an overlap of 5 SNPs. This resulted in 162,292 SNPs (PsychArray) and 176,553 SNPs (GSAchip).

Methylation

We performed basic quality control on data generated by either the 450k or EPIC arrays using Illumina's Genome Studio software for background subtraction and colour correction. Data was filtered to remove CpGs with high detection p values, those on the X or Y chromosome, or with previously identified poor performance. 450k data was normalized using SWAN and EPIC data using BMIQ, and both used ComBat to correct for chip (both), and row (450k only). Details for DNA methylation measurements and quality control have been published [62]. The final analysis was performed with 107 samples with methylation levels from the 450k array and 151 with methylation levels assessed on the EPIC array and available genotypes. Neonatal blood cell counts were estimated for seven cell types: nucleated red blood cells, granulocytes, monocytes, natural killer cells, B cells, CD4(+)T cells, and CD8(+)T cells [68].

VMRs

We identified 6,072 candidate VMRs in DCHS I and 10,005 candidate VMRs in DCHS II.

The UCI cohort

Mothers and children were part of an ongoing, longitudinal study, conducted at the University of California, Irvine (UCI), for which mothers were recruited during the first trimester of pregnancy [31-33]. All women had singleton, intrauterine pregnancies. Women were not eligible for study participation if they met the following criteria: corticosteroids, or illicit drugs during pregnancy (verified by urinary cotinine and drug toxicology). Exclusion criteria for the newborn were preterm birth (i.e., less than 34 weeks of gestational age at birth), as well as any congenital, genetic, or neurologic disorders at birth.

Ethics

The UCI institutional review board approved all study procedures and all participants provided written informed consent.

Maternal Characteristics

Maternal sociodemographic characteristics (age, parity) were obtained via a standardized structured interview at the first pregnancy visit. Maternal pre-pregnancy BMI (weight kg/height m^2) was computed based on pre-pregnancy weight abstracted from the medical record, and maternal height was measured at the research laboratory during the first pregnancy visit. Obstetric risk conditions during pregnancy, including presence of gestational diabetes and hypertension, and delivery mode were abstracted from the medical record. At each pregnancy visit the Center for Epidemiological Studies Depression Scale [59] and the State scale from the State–Trait Anxiety Inventory [60] were administered. For individuals with <3 missing items on any scale at any time point, the mean responses for that scale were calculated and then multiplied by the total number of items in the respective scale, to generate total scale scores that are comparable to those generated from participants without any missing data. We used the average depression and anxiety score throughout pregnancy in the calculations. Maternal smoking during

pregnancy was determined by maternal self-report and verified by measurement of urinary cotinine concentration. Urinary cotinine was assayed in maternal samples collected at each trimester using the Nicotine/COT(Cotinine)/Tobacco Drug Test Urine Cassette (http://www.meditests.com/nicuintescas.html), which involves transferring 4 drops of room temperature urine into the well of the cassette, and employs a cutoff for COT presence of 200ng/ml. Endorsement of smoking or detection of urinary COT in any trimester was coded as 1, and absence of evidence for smoking in any trimester coded as 0.

Genotyping

Genomic DNA was extracted from heel prick blood samples and used for all genomic analysis. Genotyping was performed on Illumina Human Omni Express (24 v1.1) Arrays containing 713,014 SNPs. All samples had a high call rate (above 97%). SNPs with a minor allele frequency >5% and a p-value for deviation from Hardy-Weinberg-Equilibrium > 1.0×10^{-25} were retained for analysis. After QC, 602,807 SNPs were available.

Imputation

Before imputation, chromosomal and base pair positions were updated to the Haplotype Reference Consortium (r1.1) reference set, allele strands were flipped where necessary. Phasing was performed using EAGLE2 (https://data.broadinstitute.org/alkesgroup/Eagle/) and imputation was performed using PBWT (https://github.com/VertebrateResequencing/pbwt). Imputed SNPs with an info score < 0.8, duplicates and ambiguous SNPs were removed resulting in 21,341,980 SNPs. All SNPs with MAF < 0.01 were removed. Of the remaining SNPs, 19,530 were DeepSEA variants.

DNA Methylation

729 DNAm analysis using the Infinium Illumina MethylationEPIC BeadChip (Illumina, Inc., San
730 Diego, CA) was performed according to the manufacturer´s guidelines in using genomic DNA
731 derived from neonatal heel prick samples. Quality Control carried out in *minfi* [61]. No outliers
732 were detected in the median intensities of methylated and unmethylated channels. All samples
733 had a high call rate of at least 95% and their predicted sex was the same as the phenotypic
734 sex. We removed CpGs with a high detection value ($p<0.0001$), probes missing >3 beads in >5%
735 of the cohort, in addition to non-specific/cross-hybridizing and SNP probes [66,67]. Methylation
736 beta-values were normalized using functional normalization (*funnorm*) [63]. We also iteratively
737 adjusted the data for relevant technical factors, i.e. array row, experimental batch and sample
738 plate, using *Combat* [64]. The final dataset contained 768,910 CpGs. Neonatal blood cell counts
739 were estimated for seven cell types: nucleated red blood cells, granulocytes, monocytes, natural
740 killer cells, B cells, CD4(+)T cells, and CD8(+)T cells [68]. The final dataset contained 121
741 samples with available genotypes and methylation values.
742 *VMRs*
743 Applying the same procedure as for PREDO I and PREDO II, we identified 9,525 candidate
744 VMRs in the ICU cohort.
745
746 *MoBa cohort*
747 Participants represent two subsets of mother-offspring pairs from the national Norwegian Mother
748 and Child Cohort Study (MoBa) [72]. MoBa is a prospective population-based pregnancy cohort
749 study conducted by the Norwegian Institute of Public Health. The years of birth for MoBa
750 participants ranged from 1999-2009. MoBa mothers provided written informed consent. Each
751 subset is referred to here as MoBa1 and MoBa2. MoBa1 is a subset of a larger study within

MoBa that included a cohort random sample and cases of asthma at age three years [73]. We previously reported an association between maternal smoking during pregnancy and differential DNA methylation in MoBa1 newborns [74]. We subsequently measured DNA methylation in additional newborns (MoBa2) in the same laboratory (Illumina, San Diego, CA) [11]. MoBa2 included cohort random sample plus cases of asthma at age seven years and non-asthmatic controls. Years of birth were 2002-2004 for children in MoBa1, 2000-2005 for MoBa2.

Ethics

The establishment and data collection in MoBa obtained a license from the Norwegian Data Inspectorate and approval from The Regional Committee for Medical Research Ethics. Both studies were approved by the Regional Committee for Ethics in Medical Research, Norway. In addition, MoBa1 and MoBa2 were approved by the Institutional Review Board of the National Institute of Environmental Health Sciences, USA.

Maternal characteristics

To replicate specific GxE and G+E from PREDO I, we focused on those characteristics which were available in both cohorts: maternal age, pre-pregnancy BMI and hypertension.

Within MoBa, the questionnaires at weeks 17 and 30 include general background information as well as details on previous and present health problems and exposures. The birth record from the Medical Birth Registry of Norway [75]which includes maternal health during pregnancy as well as procedures around birth and pregnancy outcomes, is integrated in the MoBa database.

Genotyping and Imputation

DNA was extracted from the MoBa biobank and genotyped on the Illumina HumanExomeCore platform. The genotypes were called with GenomeStudio software. Phasing and imputation were done using shapeit2 (https://mathgen.stats.ox.ac.uk./genetics_software/shapeit/shapeit.html) and

impute2 (https://mathgen.stats.ox.ac.uk/impute/impute_v2.html) with the thousand genomes phase 3 reference panel for the European population. Variants with a imputation score of less than 0.8 and with a minor allele frequency below 1% were filtered out.

Methylation

Details of the DNA methylation measurements and quality control for the MoBa1 participants were previously described [36] and the same protocol was implemented for the MoBa2 participants. Briefly, at birth, umbilical cord blood samples were collected and frozen at birth at -80°C. All biological material was obtained from the Biobank of the MoBa study [36]. Bisulfite conversion was performed using the EZ-96 DNA Methylation kit (Zymo Research Corporation, Irvine, CA) and DNA methylation was measured at 485,577 CpGs in cord blood using Illumina's Infinium HumanMethylation450 BeadChip [76]. Raw intensity (.idat) files were handled in R using the *minfi* package to calculate the methylation level at each CpG as the beta-value (β=intensity of the methylated allele (M)/(intensity of the unmethylated allele (U) + intensity of the methylated allele (M) + 100)) and the data was exported for quality control and processing. Control probes (N=65) and probes on X (N=11 230) and Y (N=416) chromosomes were excluded in both datasets. Remaining CpGs missing > 10% of methylation data were also removed (N=20 in MoBa1, none in MoBa2). Samples indicated by Illumina to have failed or have an average detection p value across all probes < 0.05 (N=49 MoBa1, N=35 MoBa2) and samples with gender mismatch (N=13 MoBa1, N=8 MoBa2) were also removed. For MoBa1 and MoBa2, we accounted for the two different probe designs by applying the intra-array normalization strategy Beta Mixture Quantile dilation (BMIQ) [77]. The Empirical Bayes method via *ComBat* was applied separately in MoBa1 and MoBa2 for batch correction using the *sva* package in R [65]. After quality control exclusions, the sample sizes were 1,068 for MoBa1 and 685 for MoBa2.

After QC, the total number of samples was 1,732, with 1,592 overlapping with the methylation samples. Specific G+E and GxE associations were calculated in the combined dataset of MoBa1 and MoBa2, while VMR analysis was conducted in MoBa1 only.

Regression analysis

Linear regression analysis was conducted using the *lm* function in R 3.3.1 (https://www.r-project.org). We included the child's sex, gestational age, seven estimated cell counts as well as the first two (PREDO I and PREDO II), first three (UCI) and first five (DCHS I and II) principal components of the MDS analysis on the genotypes in the model. The corresponding plot of the first ten MDS-components in PREDO is depicted in Figure S4. SNP genotypes were recoded into a count of 0, 1 or 2 representing the number of minor allele copies. For each VMR site, we tested SNPs located in a 1MB window up- and downstream of the specific site. In PREDO and UCI, we restricted the analysis to DeepSEA variants while we used the pruned SNP-set in DCHS.

For each VMR, we tested four models:

(1) Methylation at tagCpG ~ covariates + environment

(2) Methylation at tagCpG ~ covariates + SNP

(3) Methylation at tagCpG ~ covariates + SNP + environment

(4) Methylation at tagCpG ~ covariates + SNP + environment + SNP x environment

In model (1) we included all ten different environments, in model (2) all DeepSEA cis SNPs and in models (3) and (4) all possible environment-cis-SNP combinations. Please also see Figure 1.

For each model, the AIC, Akaike's information criterion [37] was calculated and the model with the lowest AIC was chosen as the best model. The AIC was obtained using the *AIC* function in R 3.3.1 (https://www.r-project.org).

P-values were obtained from the summary function and adjusted for the number of tested Es (E model), of tested cis SNPs (G model) or of tested cis SNP-environment combinations (G+E/GxE model) using Bonferroni-correction. Afterwards, we used FDR to correct for all tested tagCpGs (all models) using *p.adjust* in R.

Enrichment analyses

With regard to enrichment for VMRs, CpG-site within VMRs were compared to all other CpG-sites on the 450K array located in non-VMR-regions. With regard to enrichment for VMRs best explained by G, G+E or GxE, tagCpGs best explained by the specific model were compared to tagCpGs best explained by any of the other models. For enrichment tests for DeepSEA SNPs, non-DeepSEA SNPs present in our dataset were used as comparison group. Enrichment tests were performed based on a hyper-geometric test, i.e. a Fisher-test. The significance levels was set at $p<0.05$.

With regard to enrichment for GWAS hits, DeepSEA variants were matched to GWAs variants based on chromosome and position (hg19). To check for enrichment for nominal significant GWAS hits, the full summary statistics were derived from the respective publication.

Histone ChiP-seq peaks from Roadmap Epigenomics project for blood and embryonic stem cells were downloaded from http://egg2.wustl.edu/roadmap/data/byFileType/peaks/consolidated/broadPeak/.

The pre-processed consolidated broad peaks from the uniform processing pipeline of the Roadmap project were used.

Genomic annotation mapping

CpG sites were mapped to the genome location according to Illumina's annotation using the R-package *minfi*.

DeepSEA Analysis

Pretrained DeepSEA model was downloaded from: http://deepsea.princeton.edu/media/code/deepsea.v0.94.tar.gz and variant files in VCF format are used for producing e-values. VCF files were first split into smaller files each containing one million variants and the model was run using the command line on a server with a NVIDIA Titan X GPU card.

We reran our models using only DeepSEA variants which had been identified by the algorithm of Zhou and Troyanskaya [38]. This method predicts functionality of a SNP based on the DNA-sequence. We included all 212,210 variants with a functional significance e-value below $5x10^{-05}$. The e-values represent the significance of the regulatory impact of given variants compared to one million random variants.

Random-effects meta-analysis

GxE and G+E result for PREDO and for MoBa were meta-analysed using a random-effects model in the R-package rmeta. Replication was defined as DeepSEA-tagCpG-environment combinations showing the same effect direction in both cohorts, presenting with smaller p-values

as for PREDO alone and with a FDR-corrected p-value (across all combinations tested in the meta-analysis) below 0.05.

Data availability

The datasets analyzed during the current study are not publicly available. However, an interested researcher can obtain a de-identified dataset after approval from the PREDO Study Board. Data requests may be subject to further review by the national register authority and by the ethical committees. Any requests for data use should be addressed to the PREDO Study Board (predo.study@helsinki.fi) or individual researchers. The summary statistics of the best models for PREDO I are accessible at: *https:/doi.org/10.6084/m9.figshare.8074964.* For access to the UCI cohort, please contact claudia.buss@charite.de , for access to DCHS please contact Heather.Zar@uct.ac.za, for MoBa access please apply for data access at https:/www.fih.no

Acknowledgements

We want to thank Susanne Sauer and Maik Ködel for their technical assistance. We thank all mothers who took part in the on-going PREDO study. We are grateful to all the families in Norway who participate in the on-going MoBa cohort study. We thank the Drakenstein Child Health Study staff, and the clinical and administrative staff of the Western Cape Government Department of Health at Paarl Hospital and at the clinics for support of the Study. We also thank our collaborators and students. Finally, we thank all mothers and children enrolled in the Drakenstein Child Health Study. We thank the research participants and employees of 23andMe, Inc. for their contribution to this study.

887

888 ***Author's contributions***

889 DC and EBB conceived the analyses.

890 JL, MLP, EH, EK, HL, PMV, RRM and KR conceptualized and planned the PREDO study and

891 collected the data.

892 CMP, WN, SH and SJL conceptualized and planned the MoBa study and collected the data.

893 CB, SE, PWD, KJOD conceptualized and planned the UCI study and collected the data.

894 DTSL and JLM performed the DNA methylation and genotyping arrays for the UCI and DCH

895 studies.

896 DJS, NK, HJZ designed and undertook the DCHS; MJM, MSK, KCK were involved in testing

897 and analysis of epigenetic data; SD was involved in testing and analysis of genetic data.

898 DC, GE, CMP and MJJ ran the statistical analysis.

899 NSM, IK and FJT co-supervised statistical analysis.

900 DC and EBB wrote the manuscript with contributions from GE, SJL, CMP, KR, JL.

901 DC, JL, KR, and EB interpreted the results.

902 All authors contributed to and approved the final version of the manuscript.

903

904 ***Competing interests***

905 DC, GE, JL, CMP, MLP, EH, EK, HL, PMV, RMR, WN, SH, SJL, KJOD, EG, MJM, SE, PDW,

906 CB, MJJ, DTSL, JLMI, MSK, NK, HJZ, KCK, SD, DJS, IK, NSM, FJT, KR have no competing

907 interests. EBB is co-inventor on the following patent applications: FKBP5: a novel target for

908 antidepressant therapy. European Patent# EP 1687443 B1; Polymorphisms in ABCB1 associated

909 with a lack of clinical response to medicaments. United States Patent # 8030033; Means and

methods for diagnosing predisposition for treatment emergent suicidal ideation (TESI). European application number: 08016477.5 International application number: PCT/EP2009/061575.

Funding

This work was supported by the Academy of Finland (EK, HL, KR, JL); University of Helsinki Research Funds (JL, MLP,HL), British Heart Foundation (RMR); Tommy's (RMR); European Commission (EK, KR, Horizon 2020 Award SC1-2016-RTD-733280 RECAP); NorFace DIAL (EK, KR PremLife); Foundation for Pediatric Research (EK); Juho Vainio Foundation (EK); Novo Nordisk Foundation (EK); Signe and Ane Gyllenberg Foundation (EK, KR); Sigrid Jusélius Foundation (EK); Finnish Medical Foundation (HL); Jane and Aatos Erkko Foundation (HL); Päivikki and Sakari Sohlberg Foundation (HL, PMV); the Clinical Graduate school in Pediatrics and Obstetrics/Gynaecology in University of Helsinki (PMV). The Norwegian Mother and Child Cohort Study is supported by the Norwegian Ministry of Health and Care Services and the Ministry of Education and Research, NIH/NIEHS (contract no N01-ES-75558), NIH/NINDS (grant no.1 UO1 NS 047537-01 and grant no.2 UO1 NS 047537-06A1). For this work, MoBa 1 and 2 were supported by the Intramural Research Program of the NIH, National Institute of Environmental Health Sciences (Z01-ES-49019) and the Norwegian Research Council/BIOBANK (grant no 221097). This work was also partly supported by the Research Council of Norway through its Centres of Excellence funding scheme, project number 262700. The Drakenstein Child Health Study is supported by the Bill and Melinda Gates Foundation (OPP 1017641); with additional support for this work from the Eunice Kennedy Shriver National Institute of Child Health and Human Development of the National Institutes of Health (NICHD) under Award Number R21HD085849; and the Fogarty International Center (FIC). The content

933 is solely the responsibility of the authors and does not necessarily represent the official views of
934 the National Institutes of Health. Additional support for HJZ, DJS and NK, and for research
935 reported in this publication was by the South African Medical Research Council (SAMRC); NK
936 receives support from the SAMRC under a Self-Initiated Research Grant. The views and
937 opinions expressed are those of the authors and do not necessarily represent the official views of
938 the SAMRC.
939 This work was also funded by the German Federal Ministry of Education and Research through
940 the Research Consortium Integrated Network IntegraMent (grant 01ZX1314H) under the
941 auspices of the e:Med Programme (NSM).
942 The UCI cohort was supported by a European Research Area Network (ERA Net) Neuron grant
943 (01EW1407A, CB) and National Institutes of Health grant (R01 HD-060628, CB) as well as NIH
944 grant R01 MH-105538 (PDW).
945 This work was also funded by the Canadian Institute for Advanced Research, Child and Brain
946 Development Program, Toronto, ON, Canada (KJOD).
947

948 ***Figures and figure legends***
949
950 Figure 1: Flow diagram of VMR analysis
951
952 Figure 2: VMR-analysis in pruned PREDO I dataset
953
954 A: Percentage of models (G, E, GxE or G+E) with the lowest AIC explaining variable DNA
955 methylation using the PREDO I dataset with pruned SNPs.
956
957 B: Distribution of the different types of prenatal environment included in the E model with the
958 lowest AIC (right), in the combinations yielding the best model GxE (middle), or the best model
959 G+E models (left). To increase readability all counts < 3% have been omitted.
960
961 C: DeltaAIC, i.e , the difference in AIC, between best model and next best model, stratified by
962 the best model. Y-axis denotes the delta AIC and the X-axis the different models. The median is
963 depicted by a black line, the rectangle spans the first quartile to the third quartile, whiskers above

and below the box show the location of minimum and maximum beta-values. P-values are based on Wilcoxon-tests.

Figure 3: VMR-analysis in DeepSEA annotated SNPs in PREDO I dataset.

A: Percentage of models (G, E, GxE or G+E) with the lowest AIC explaining variable DNA methylation using the PREDO I dataset with DeepSEA annotated SNPs.

B: Distribution of the locations of all VMRs and tagVMRs with best model E, G, G+E and GxE on the 450k array using only DeepSEA variants in relationship to CpG-Islands based on the Illumina 450K annotation.

C: Distribution of gene-centric locations of all VMRs and tagVMRs with best model E, G, G+E and GxE on the 450k array using only DeepSEA variants.

Figure 4: Functional annotation of VMR-mapping in DeepSEA annotated SNPs in PREDO I dataset

A: Histone mark enrichment for all VMRs. The Y-axis denotes the fold enrichment/depletion as compared to no-VMRs. Blue bars indicate significant enrichment/depletion, grey bars non-significant differences based on Fisher-tests.

B: Histone mark enrichment for tagVMRs with best model E, G, G+E and GxE relative to all VMRs. Green color indicates depletion, red color indicates enrichment. Thick black lines around the rectangles indicate significant enrichment/depletion based on Fisher-tests.

C: Histone mark enrichment for all DeepSEA variants in the dataset. Blue bars indicate significant enrichment/depletion based on Fisher-tests.

D: Histone mark enrichment for all DeepSEA variants involved in models where either G, G+E or GxE is the best model as compared to all tested DeepSEA variants. Green color indicates depletion, red color indicates enrichment. Thick black lines around the rectangles indicate significant enrichment/depletion based on Fisher-tests.

Figure 5: VMR-analysis in PREDO I and replication datasets

Percentage of models (G, E, GxE or G+E) with the lowest AIC explaining variable DNA methylation in PREDO I (450K), DCHS I (450K), PREDO II (EPIC), UCI (EPIC) and DCHS II (EPIC)

Figure 6: Consistency of best models across cohorts

Percentage of consistent best models in overlapping tag CpGs of PREDO I (450K), DCHS I (450K), PREDO II (EPIC), UCI (EPIC) and DCHS II (EPIC). Overlapping VMRs included significantly more CpGs as compared to all VMRs ($p<2.2x10^{-16}$, Wilcoxon-test, mean=4.43).

Figure 7: Enrichment of DeepSEA variants for GWAS associations

A: Enrichment for nominal significant GWAS associations for all tested DeepSEA variants and their LD proxies for GWAS for ADHD (attention deficit hyperactivity disorder), ASD (autism spectrum disorder), BMI (body-mass index), BP (bipolar disorder), CrossDisorder, IBD (inflammatory bowel disease), MDD (major depressive disorder), SCZ (schizophrenia) and T2D (Type 2 diabetes).
The Y-axis denotes the fold enrichment with regard to non-DeepSEAvariants. Blue bars indicate significant enrichment/depletion based on Fisher-tests.

B: Enrichment for nominal significant GWAS hits for DeepSEA variants and their LD proxies involved in best models with G, G+E or GxE as compared to all tested DeepSEA variants. Green color indicates depletion, red color indicates enrichment. Thick black lines around the rectangles indicate significant enrichment/depletion based on Fisher-tests.

Bibliography

1 Roseboom, T., de Rooij, S. & Painter, R. The Dutch famine and its long-term consequences for adult health. *Early Hum Dev* **82**, 485-491, doi:10.1016/j.earlhumdev.2006.07.001 (2006).

2 Barker, D. J., Osmond, C., Forsen, T. J., Kajantie, E. & Eriksson, J. G. Trajectories of growth among children who have coronary events as adults. *N Engl J Med* **353**, 1802-1809, doi:10.1056/NEJMoa044160 (2005).

3 Hovi, P. *et al.* Glucose regulation in young adults with very low birth weight. *N Engl J Med* **356**, 2053-2063, doi:10.1056/NEJMoa067187 (2007).

4 Hillier, T. A. *et al.* Childhood obesity and metabolic imprinting: the ongoing effects of maternal hyperglycemia. *Diabetes Care* **30**, 2287-2292, doi:10.2337/dc06-2361 (2007).

5 Dancause, K. N. *et al.* Prenatal stress due to a natural disaster predicts adiposity in childhood: the Iowa Flood Study. *J Obes* **2015**, 570541, doi:10.1155/2015/570541 (2015).

6 Lahti, M. *et al.* Maternal Depressive Symptoms During and After Pregnancy and Psychiatric Problems in Children. *J Am Acad Child Adolesc Psychiatry* **56**, 30-39 e37, doi:10.1016/j.jaac.2016.10.007 (2017).

7 Bronson, S. L. & Bale, T. L. The Placenta as a Mediator of Stress Effects on Neurodevelopmental Reprogramming. *Neuropsychopharmacology* **41**, 207-218, doi:10.1038/npp.2015.231 (2016).

8 Schwarze, C. E. *et al.* Prenatal adversity: a risk factor in borderline personality disorder? *Psychol Med* **43**, 1279-1291, doi:10.1017/S0033291712002140 (2013).

9 Entringer, S., Buss, C. & Wadhwa, P. D. Prenatal stress, development, health and disease risk: A psychobiological perspective-2015 Curt Richter Award Paper. *Psychoneuroendocrinology* **62**, 366-375, doi:10.1016/j.psyneuen.2015.08.019 (2015).

10 Gutierrez-Arcelus, M. *et al.* Passive and active DNA methylation and the interplay with genetic variation in gene regulation. *Elife* **2**, e00523, doi:10.7554/eLife.00523 (2013).

11 Joubert, B. R. *et al.* DNA Methylation in Newborns and Maternal Smoking in Pregnancy: Genome-wide Consortium Meta-analysis. *Am J Hum Genet* **98**, 680-696, doi:10.1016/j.ajhg.2016.02.019 (2016).

12 Sharp, G. C. *et al.* Maternal BMI at the start of pregnancy and offspring epigenome-wide DNA methylation: findings from the pregnancy and childhood epigenetics (PACE) consortium. *Hum Mol Genet* **26**, 4067-4085, doi:10.1093/hmg/ddx290 (2017).

13 Girchenko, P. *et al.* Associations between maternal risk factors of adverse pregnancy and birth outcomes and the offspring epigenetic clock of gestational age at birth. *Clin Epigenetics* **9**, 49, doi:10.1186/s13148-017-0349-z (2017).

14 Rijlaarsdam, J. *et al.* An epigenome-wide association meta-analysis of prenatal maternal stress in neonates: A model approach for replication. *Epigenetics* **11**, 140-149, doi:10.1080/15592294.2016.1145329 (2016).

15 Sosnowski, D. W., Booth, C., York, T. P., Amstadter, A. B. & Kliewer, W. Maternal prenatal stress and infant DNA methylation: A systematic review. *Dev Psychobiol* **60**, 127-139, doi:10.1002/dev.21604 (2018).

16 Bauer, T. *et al.* Environment-induced epigenetic reprogramming in genomic regulatory elements in smoking mothers and their children. *Mol Syst Biol* **12**, 861, doi:10.15252/msb.20156520 (2016).

17 Sharp, G. C. *et al.* Maternal pre-pregnancy BMI and gestational weight gain, offspring DNA methylation and later offspring adiposity: findings from the Avon Longitudinal Study of Parents and Children. *Int J Epidemiol* **44**, 1288-1304, doi:10.1093/ije/dyv042 (2015).
18 Lin, X. *et al.* Developmental pathways to adiposity begin before birth and are influenced by genotype, prenatal environment and epigenome. *BMC Med* **15**, 50, doi:10.1186/s12916-017-0800-1 (2017).
19 Cecil, C. A. *et al.* DNA methylation and substance-use risk: a prospective, genome-wide study spanning gestation to adolescence. *Transl Psychiatry* **6**, e976, doi:10.1038/tp.2016.247 (2016).
20 Gibbs, J. R. *et al.* Abundant quantitative trait loci exist for DNA methylation and gene expression in human brain. *PLoS Genet* **6**, e1000952, doi:10.1371/journal.pgen.1000952 (2010).
21 Gaunt, T. R. *et al.* Systematic identification of genetic influences on methylation across the human life course. *Genome Biol* **17**, 61, doi:10.1186/s13059-016-0926-z (2016).
22 McClay, J. L. *et al.* High density methylation QTL analysis in human blood via next-generation sequencing of the methylated genomic DNA fraction. *Genome Biol* **16**, 291, doi:10.1186/s13059-015-0842-7 (2015).
23 Chen, L. *et al.* Genetic Drivers of Epigenetic and Transcriptional Variation in Human Immune Cells. *Cell* **167**, 1398-1414 e1324, doi:10.1016/j.cell.2016.10.026 (2016).
24 Hannon, E., Weedon, M., Bray, N., O'Donovan, M. & Mill, J. Pleiotropic Effects of Trait-Associated Genetic Variation on DNA Methylation: Utility for Refining GWAS Loci. *Am J Hum Genet* **100**, 954-959, doi:10.1016/j.ajhg.2017.04.013 (2017).
25 Pierce, B. L. *et al.* Co-occurring expression and methylation QTLs allow detection of common causal variants and shared biological mechanisms. *Nat Commun* **9**, 804, doi:10.1038/s41467-018-03209-9 (2018).
26 Cheung, W. A. *et al.* Functional variation in allelic methylomes underscores a strong genetic contribution and reveals novel epigenetic alterations in the human epigenome. *Genome Biol* **18**, 50, doi:10.1186/s13059-017-1173-7 (2017).
27 Gluckman, P. D., Hanson, M. A., Cooper, C. & Thornburg, K. L. Effect of in utero and early-life conditions on adult health and disease. *N Engl J Med* **359**, 61-73, doi:10.1056/NEJMra0708473 (2008).
28 Klengel, T. *et al.* Allele-specific FKBP5 DNA demethylation mediates gene-childhood trauma interactions. *Nat Neurosci* **16**, 33-41, doi:10.1038/nn.3275 (2013).
29 Teh, A. L. *et al.* The effect of genotype and in utero environment on interindividual variation in neonate DNA methylomes. *Genome Res* **24**, 1064-1074, doi:10.1101/gr.171439.113 (2014).
30 Girchenko, P. *et al.* Prediction and Prevention of Preeclampsia and Intrauterine Growth Restriction (PREDO) study. *International journal of epidemiology*, doi:10.1093/ije/dyw154 (2016).
31 Graham, A. M. *et al.* Maternal Systemic Interleukin-6 During Pregnancy Is Associated With Newborn Amygdala Phenotypes and Subsequent Behavior at 2 Years of Age. *Biol Psychiatry* **83**, 109-119, doi:10.1016/j.biopsych.2017.05.027 (2018).
32 Moog, N. K. *et al.* Intergenerational Effect of Maternal Exposure to Childhood Maltreatment on Newborn Brain Anatomy. *Biol Psychiatry* **83**, 120-127, doi:10.1016/j.biopsych.2017.07.009 (2018).

33 Entringer, S. *et al.* Maternal Cortisol During Pregnancy and Infant Adiposity: A Prospective Investigation. *J Clin Endocrinol Metab* **102**, 1366-1374, doi:10.1210/jc.2016-3025 (2017).
34 Stein, D. J. *et al.* Investigating the psychosocial determinants of child health in Africa: The Drakenstein Child Health Study. *J Neurosci Methods* **252**, 27-35, doi:10.1016/j.jneumeth.2015.03.016 (2015).
35 Zar, H. J., Barnett, W., Myer, L., Stein, D. J. & Nicol, M. P. Investigating the early-life determinants of illness in Africa: the Drakenstein Child Health Study. *Thorax* **70**, 592-594, doi:10.1136/thoraxjnl-2014-206242 (2015).
36 Ronningen, K. S. *et al.* The biobank of the Norwegian Mother and Child Cohort Study: a resource for the next 100 years. *Eur J Epidemiol* **21**, 619-625, doi:10.1007/s10654-006-9041-x (2006).
37 Akaike, H. in *Proceedings of the Second International Symposium on Information Theory (ed.* 267–281 (Akademiai Kiado, 1973
).
38 Zhou, J. & Troyanskaya, O. G. Predicting effects of noncoding variants with deep learning-based sequence model. *Nat Methods* **12**, 931-934, doi:10.1038/nmeth.3547 (2015).
39 Consortium, E. P. The ENCODE (ENCyclopedia Of DNA Elements) Project. *Science* **306**, 636-640, doi:10.1126/science.1105136 (2004).
40 Autism Spectrum Disorders Working Group of The Psychiatric Genomics, C. Meta-analysis of GWAS of over 16,000 individuals with autism spectrum disorder highlights a novel locus at 10q24.32 and a significant overlap with schizophrenia. *Mol Autism* **8**, 21, doi:10.1186/s13229-017-0137-9 (2017).
41 Demontis, D. *et al.* Discovery of the first genome-wide significant risk loci for attention deficit/hyperactivity disorder. *Nat Genet* **51**, 63-75, doi:10.1038/s41588-018-0269-7 (2019).
42 Psychiatric, G. C. B. D. W. G. Large-scale genome-wide association analysis of bipolar disorder identifies a new susceptibility locus near ODZ4. *Nat Genet* **43**, 977-983, doi:10.1038/ng.943 (2011).
43 Wray, N. R. *et al.* Genome-wide association analyses identify 44 risk variants and refine the genetic architecture of major depression. *Nat Genet* **50**, 668-681, doi:10.1038/s41588-018-0090-3 (2018).
44 Schizophrenia Working Group of the Psychiatric Genomics, C. Biological insights from 108 schizophrenia-associated genetic loci. *Nature* **511**, 421-427, doi:10.1038/nature13595 (2014).
45 Cross-Disorder Group of the Psychiatric Genomics, C. Identification of risk loci with shared effects on five major psychiatric disorders: a genome-wide analysis. *Lancet* **381**, 1371-1379, doi:10.1016/S0140-6736(12)62129-1 (2013).
46 Liu, J. Z. *et al.* Association analyses identify 38 susceptibility loci for inflammatory bowel disease and highlight shared genetic risk across populations. *Nat Genet* **47**, 979-986, doi:10.1038/ng.3359 (2015).
47 Morris, A. P. *et al.* Large-scale association analysis provides insights into the genetic architecture and pathophysiology of type 2 diabetes. *Nat Genet* **44**, 981-990, doi:10.1038/ng.2383 (2012).

48 Horikoshi, M. *et al.* Discovery and Fine-Mapping of Glycaemic and Obesity-Related Trait Loci Using High-Density Imputation. *PLoS Genet* **11**, e1005230, doi:10.1371/journal.pgen.1005230 (2015).
49 Sandoval, J. *et al.* Validation of a DNA methylation microarray for 450,000 CpG sites in the human genome. *Epigenetics* **6**, 692-702 (2011).
50 Mehta, D. *et al.* Childhood maltreatment is associated with distinct genomic and epigenetic profiles in posttraumatic stress disorder. *Proc Natl Acad Sci U S A* **110**, 8302-8307, doi:10.1073/pnas.1217750110 (2013).
51 Grishkevich, V., Yanai, I. The genomic determinants of genotype × environment interactions in gene expression. *Trends in Genetics* **29**, 479-487 (2013).
52 Grishkevich, V. *et al.* A genomic bias for genotype-environment interactions in C. elegans. *Mol Syst Biol* **8**, 587, doi:10.1038/msb.2012.19 (2012).
53 Chen, Y. A. *et al.* Discovery of cross-reactive probes and polymorphic CpGs in the Illumina Infinium HumanMethylation450 microarray. *Epigenetics* **8**, 203-209, doi:10.4161/epi.23470 (2013).
54 Ong, M. L. & Holbrook, J. D. Novel region discovery method for Infinium 450K DNA methylation data reveals changes associated with aging in muscle and neuronal pathways. *Aging Cell* **13**, 142-155, doi:10.1111/acel.12159 (2014).
55 Gu, J. *et al.* Mapping of Variable DNA Methylation Across Multiple Cell Types Defines a Dynamic Regulatory Landscape of the Human Genome. *G3 (Bethesda)* **6**, 973-986, doi:10.1534/g3.115.025437 (2016).
56 Feinberg, A. P. & Irizarry, R. A. Evolution in health and medicine Sackler colloquium: Stochastic epigenetic variation as a driving force of development, evolutionary adaptation, and disease. *Proc Natl Acad Sci U S A* **107 Suppl 1**, 1757-1764, doi:10.1073/pnas.0906183107 (2010).
57 Elliott, G. *et al.* Intermediate DNA methylation is a conserved signature of genome regulation. *Nat Commun* **6**, 6363, doi:10.1038/ncomms7363 (2015).
58 Zhang, P. Inference after variable selection in linear regression models. *Biometrika* **79**, 741–746 (1992).
59 Radloff, L. S. The CES-D Scale: A Self-Report Depression Scale for Research in the General Population. *Appl Psychol Meas* **1**, 385-401 (1977).
60 Spielberger, C. D. *State-Trait Anxiety Inventory: Bibliography*. 2nd Edition edn, (Consulting Psychologists Press, 1989).
61 Aryee, M. J. *et al.* Minfi: a flexible and comprehensive Bioconductor package for the analysis of Infinium DNA methylation microarrays. *Bioinformatics* **30**, 1363-1369, doi:10.1093/bioinformatics/btu049 (2014).
62 Morin, A. M. *et al.* Maternal blood contamination of collected cord blood can be identified using DNA methylation at three CpGs. *Clin Epigenetics* **9**, 75, doi:10.1186/s13148-017-0370-2 (2017).
63 Fortin, J. P. *et al.* Functional normalization of 450k methylation array data improves replication in large cancer studies. *Genome Biol* **15**, 503, doi:10.1186/s13059-014-0503-2 (2014).
64 Johnson, W. E., Li, C. & Rabinovic, A. Adjusting batch effects in microarray expression data using empirical Bayes methods. *Biostatistics* **8**, 118-127, doi:10.1093/biostatistics/kxj037 (2007).

65 Leek, J. T., Johnson, W. E., Parker, H. S., Jaffe, A. E. & Storey, J. D. The sva package for removing batch effects and other unwanted variation in high-throughput experiments. *Bioinformatics* **28**, 882-883, doi:10.1093/bioinformatics/bts034 (2012).
66 Price, M. E. *et al.* Additional annotation enhances potential for biologically-relevant analysis of the Illumina Infinium HumanMethylation450 BeadChip array. *Epigenetics Chromatin* **6**, 4, doi:10.1186/1756-8935-6-4 (2013).
67 McCartney, D. L. *et al.* Identification of polymorphic and off-target probe binding sites on the Illumina Infinium MethylationEPIC BeadChip. *Genom Data* **9**, 22-24, doi:10.1016/j.gdata.2016.05.012 (2016).
68 Bakulski, K. M. *et al.* DNA methylation of cord blood cell types: Applications for mixed cell birth studies. *Epigenetics* **11**, 354-362, doi:10.1080/15592294.2016.1161875 (2016).
69 van der Westhuizen, C., Wyatt, G., Williams, J. K., Stein, D. J. & Sorsdahl, K. Validation of the Self Reporting Questionnaire 20-Item (SRQ-20) for Use in a Low- and Middle-Income Country Emergency Centre Setting. *Int J Ment Health Addict* **14**, 37-48, doi:10.1007/s11469-015-9566-x (2016).
70 Beck, A. T., Ward, C. H., Mendelson, M., Mock, J. & Erbaugh, J. An inventory for measuring depression. *Arch Gen Psychiatry* **4**, 561-571 (1961).
71 Group, W. A. W. The Alcohol, Smoking and Substance Involvement Screening Test (ASSIST): development, reliability and feasibility. *Addiction* **97**, 1183-1194 (2002).
72 Magnus, P. *et al.* Cohort Profile Update: The Norwegian Mother and Child Cohort Study (MoBa). *Int J Epidemiol* **45**, 382-388, doi:10.1093/ije/dyw029 (2016).
73 Haberg, S. E. *et al.* Maternal folate levels in pregnancy and asthma in children at age 3 years. *J Allergy Clin Immunol* **127**, 262-264, 264 e261, doi:10.1016/j.jaci.2010.10.004 (2011).
74 Joubert, B. R. *et al.* 450K epigenome-wide scan identifies differential DNA methylation in newborns related to maternal smoking during pregnancy. *Environ Health Perspect* **120**, 1425-1431, doi:10.1289/ehp.1205412 (2012).
75 Irgens, L. M. The Medical Birth Registry of Norway. Epidemiological research and surveillance throughout 30 years. *Acta Obstet Gynecol Scand* **79**, 435-439 (2000).
76 Bibikova, M. *et al.* High density DNA methylation array with single CpG site resolution. *Genomics* **98**, 288-295, doi:10.1016/j.ygeno.2011.07.007 (2011).
77 Teschendorff, A. E. *et al.* A beta-mixture quantile normalization method for correcting probe design bias in Illumina Infinium 450 k DNA methylation data. *Bioinformatics* **29**, 189-196, doi:10.1093/bioinformatics/bts680 (2013).

Listing of Psychiatric Genomics Consortium Members

Major Depressive Disorder Working Group

Naomi R Wray* 1, 2
Stephan Ripke* 3, 4, 5
Manuel Mattheisen* 6, 7, 8, 9
Maciej Trzaskowski* 1
Enda M Byrne 1
Abdel Abdellaoui 10

1. Institute for Molecular Bioscience, The University of Queensland, Brisbane, QLD, AU
2. Queensland Brain Institute, The University of Queensland, Brisbane, QLD, AU
3. Analytic and Translational Genetics Unit, Massachusetts General Hospital, Boston, MA, US
4. Department of Psychiatry and Psychotherapy, Universitätsmedizin Berlin Campus Charité Mitte, Berlin, DE
5. Medical and Population Genetics, Broad Institute, Cambridge, MA, US
6. Centre for Psychiatry Research, Department of Clinical Neuroscience, Karolinska Institutet, Stockholm, SE
7. Department of Biomedicine, Aarhus University, Aarhus, DK
8. iSEQ, Centre for Integrative Sequencing, Aarhus University, Aarhus, DK
9. iPSYCH, The Lundbeck Foundation Initiative for Integrative Psychiatric Research,, DK
10. Dept of Biological Psychology & EMGO+ Institute for Health and Care Research, Vrije Universiteit Amsterdam, Amsterdam, NL
11. Division of Psychiatry, University of Edinburgh, Edinburgh, GB
12. Centre for Integrated Register-based Research, Aarhus University, Aarhus, DK
13. National Centre for Register-Based Research, Aarhus University, Aarhus, DK
14. Discipline of Psychiatry, University of Adelaide, Adelaide, SA, AU
15. Department of Translational Research in Psychiatry, Max Planck Institute of Psychiatry, Munich, DE
16. Munich Cluster for Systems Neurology (SyNergy), Munich, DE
17. Department of Psychiatry, Virginia Commonwealth University, Richmond, VA, US
18. Center for Neonatal Screening, Department for Congenital Disorders, Statens Serum Institut, Copenhagen, DK
19. Department of Psychiatry, Vrije Universiteit Medical Center and GGZ inGeest, Amsterdam, NL
20. Virginia Institute for Psychiatric and Behavior Genetics, Richmond, VA, US
21. Department of Psychiatry and Behavioral Sciences, Emory University School of Medicine, Atlanta, GA, US
22. Department of Medical Epidemiology and Biostatistics, Karolinska Institutet, Stockholm, SE
23. Department of Clinical Medicine, Translational Neuropsychiatry Unit, Aarhus University, Aarhus, DK
24. Human Genetics, Wellcome Trust Sanger Institute, Cambridge, GB
25. Statistical genomics and systems genetics, European Bioinformatics Institute (EMBL-EBI), Cambridge, GB
26. Department of Psychiatry, University Hospital of Lausanne, Prilly, Vaud, CH
27. Social Genetic and Developmental Psychiatry Centre, King's College London, London, GB
28. Genetics and Computational Biology, QIMR Berghofer Medical Research Institute, Brisbane, QLD, AU
29. Centre for Advanced Imaging, The University of Queensland, Brisbane, QLD, AU
30. Psychological Medicine, Cardiff University, Cardiff, GB
31. Center for Genomic and Computational Biology, Duke University, Durham, NC, US
32. Department of Pediatrics, Division of Medical Genetics, Duke University, Durham, NC, US
33. Centre for Cognitive Ageing and Cognitive Epidemiology, University of Edinburgh, Edinburgh, GB
34. Institute of Human Genetics, University of Bonn, Bonn, DE

35. Life&Brain Center, Department of Genomics, University of Bonn, Bonn, DE
36. Epidemiology, Erasmus MC, Rotterdam, Zuid-Holland, NL
37. Psychiatry, Dokuz Eylul University School Of Medicine, Izmir, TR
38. Department of Psychiatry, Massachusetts General Hospital, Boston, MA, US
39. Psychiatric and Neurodevelopmental Genetics Unit (PNGU), Massachusetts General Hospital, Boston, MA, US
40. Stanley Center for Psychiatric Research, Broad Institute, Cambridge, MA, US
41. Neuroscience and Mental Health, Cardiff University, Cardiff, GB
42. Bioinformatics, University of British Columbia, Vancouver, BC, CA
43. Department of Epidemiology, Harvard T.H. Chan School of Public Health, Boston, MA, US
44. Department of Mathematics, Massachusetts Institute of Technology, Cambridge, MA, US
45. Department of Psychiatry (UPK), University of Basel, Basel, CH
46. Human Genomics Research Group, Department of Biomedicine, University of Basel, Basel, CH
47. Department of Genetic Epidemiology in Psychiatry, Central Institute of Mental Health, Medical Faculty Mannheim, Heidelberg University, Mannheim, Baden-Württemberg, DE
48. Department of Psychiatry, Trinity College Dublin, Dublin, IE
49. Psychiatry & Behavioral Sciences, Johns Hopkins University, Baltimore, MD, US
50. Bioinformatics Research Centre, Aarhus University, Aarhus, DK
51. Institute of Genetic Medicine, Newcastle University, Newcastle upon Tyne, GB
52. Danish Headache Centre, Department of Neurology, Rigshospitalet, Glostrup, DK
53. Institute of Biological Psychiatry, Mental Health Center Sct. Hans, Mental Health Services Capital Region of Denmark, Copenhagen, DK
54. iPSYCH, The Lundbeck Foundation Initiative for Psychiatric Research, Copenhagen, DK
55. Brain and Mind Centre, University of Sydney, Sydney, NSW, AU
56. Interfaculty Institute for Genetics and Functional Genomics, Department of Functional Genomics, University Medicine and Ernst Moritz Arndt University Greifswald, Greifswald, Mecklenburg-Vorpommern, DE
57. Roche Pharmaceutical Research and Early Development, Pharmaceutical Sciences, Roche Innovation Center Basel, F. Hoffmann-La Roche Ltd, Basel, CH
58. Max Planck Institute of Psychiatry, Munich, DE
59. MRC Centre for Neuropsychiatric Genetics and Genomics, Cardiff University, Cardiff, GB
60. Department of Psychological Medicine, University of Worcester, Worcester, GB
61. Division of Research, Kaiser Permanente Northern California, Oakland, CA, US
62. Psychiatry & The Behavioral Sciences, University of Southern California, Los Angeles, CA, US
63. Department of Biomedical Informatics, Harvard Medical School, Boston, MA, US
64. Department of Medicine, Brigham and Women's Hospital, Boston, MA, US
65. Informatics Program, Boston Children's Hospital, Boston, MA, US
66. Wellcome Trust Centre for Human Genetics, University of Oxford, Oxford, GB
67. Department of Endocrinology at Herlev University Hospital, University of Copenhagen, Copenhagen, DK
68. Institute of Social and Preventive Medicine (IUMSP), University Hospital of Lausanne, Lausanne, VD, CH
69. Swiss Institute of Bioinformatics, Lausanne, VD, CH
70. Division of Psychiatry, Centre for Clinical Brain Sciences, University of Edinburgh, Edinburgh, GB
71. Mental Health, NHS 24, Glasgow, GB
72. Department of Psychiatry and Psychotherapy, University of Bonn, Bonn, DE

73. Statistics, University of Oxford, Oxford, GB
74. Psychiatry, Columbia University College of Physicians and Surgeons, New York, NY, US
75. School of Psychology and Counseling, Queensland University of Technology, Brisbane, QLD, AU
76. Child and Youth Mental Health Service, Children's Health Queensland Hospital and Health Service, South Brisbane, QLD, AU
77. Child Health Research Centre, University of Queensland, Brisbane, QLD, AU
78. Estonian Genome Center, University of Tartu, Tartu, EE
79. Medical Genetics, University of British Columbia, Vancouver, BC, CA
80. Statistics, University of British Columbia, Vancouver, BC, CA
81. DZHK (German Centre for Cardiovascular Research), Partner Site Greifswald, University Medicine, University Medicine Greifswald, Greifswald, Mecklenburg-Vorpommern, DE
82. Institute of Clinical Chemistry and Laboratory Medicine, University Medicine Greifswald, Greifswald, Mecklenburg-Vorpommern, DE
83. Institute of Health and Biomedical Innovation, Queensland University of Technology, Brisbane, QLD, AU
84. Humus, Reykjavik, IS
85. Virginia Institute for Psychiatric & Behavioral Genetics, Virginia Commonwealth University, Richmond, VA, US
86. Clinical Genetics, Vrije Universiteit Medical Center, Amsterdam, NL
87. Complex Trait Genetics, Vrije Universiteit Amsterdam, Amsterdam, NL
88. Solid Biosciences, Boston, MA, US
89. Department of Psychiatry, Washington University in Saint Louis School of Medicine, Saint Louis, MO, US
90. Department of Biochemistry and Molecular Biology II, Institute of Neurosciences, Center for Biomedical Research, University of Granada, Granada, ES
91. Department of Psychiatry, University of Groningen, University Medical Center Groningen, Groningen, NL
92. Department of Psychiatry and Psychotherapy, Medical Center of the University of Munich, Campus Innenstadt, Munich, DE
93. Institute of Psychiatric Phenomics and Genomics (IPPG), Medical Center of the University of Munich, Campus Innenstadt, Munich, DE
94. Division of Cancer Epidemiology and Genetics, National Cancer Institute, Bethesda, MD, US
95. Behavioral Health Services, Kaiser Permanente Washington, Seattle, WA, US
96. Faculty of Medicine, Department of Psychiatry, University of Iceland, Reykjavik, IS
97. School of Medicine and Dentistry, James Cook University, Townsville, QLD, AU
98. Institute of Health and Wellbeing, University of Glasgow, Glasgow, GB
99. deCODE Genetics / Amgen, Reykjavik, IS
100. College of Biomedical and Life Sciences, Cardiff University, Cardiff, GB
101. Institute of Epidemiology and Social Medicine, University of Münster, Münster, Nordrhein-Westfalen, DE
102. Institute for Community Medicine, University Medicine Greifswald, Greifswald, Mecklenburg-Vorpommern, DE
103. Department of Psychiatry, University of California, San Diego, San Diego, CA, US
104. KG Jebsen Centre for Psychosis Research, Norway Division of Mental Health and Addiction, Oslo University Hospital, Oslo, NO
105. Medical Genetics Section, CGEM, IGMM, University of Edinburgh, Edinburgh, GB
106. Clinical Neurosciences, University of Cambridge, Cambridge, GB
107. Internal Medicine, Erasmus MC, Rotterdam, Zuid-Holland, NL

108. Roche Pharmaceutical Research and Early Development, Neuroscience, Ophthalmology and Rare Diseases Discovery & Translational Medicine Area, Roche Innovation Center Basel, F. Hoffmann-La Roche Ltd, Basel, CH
109. Department of Psychiatry and Psychotherapy, University Medicine Greifswald, Greifswald, Mecklenburg-Vorpommern, DE
110. Department of Psychiatry, Leiden University Medical Center, Leiden, NL
111. Virginia Institute for Psychiatric & Behavioral Genetics, Virginia Commonwealth University, Richmond, VA, US
112. Computational Sciences Center of Emphasis, Pfizer Global Research and Development, Cambridge, MA, US
113. Institute for Molecular Bioscience; Queensland Brain Institute, The University of Queensland, Brisbane, QLD, AU
114. Department of Psychiatry, University of Münster, Münster, Nordrhein-Westfalen, DE
115. Institute of Medical Genetics and Pathology, University Hospital Basel, University of Basel, Basel, CH
116. Institute of Neuroscience and Medicine (INM-1), Research Center Juelich, Juelich, DE
117. Amsterdam Public Health Institute, Vrije Universiteit Medical Center, Amsterdam, NL
118. Centre for Integrative Biology, Università degli Studi di Trento, Trento, Trentino-Alto Adige, IT
119. Department of Psychiatry and Psychotherapy, Medical Center, University of Freiburg, Faculty of Medicine, University of Freiburg, Freiburg, DE
120. Psychiatry, Kaiser Permanente Northern California, San Francisco, CA, US
121. Medical Research Council Human Genetics Unit, Institute of Genetics and Molecular Medicine, University of Edinburgh, Edinburgh, GB
122. Department of Psychiatry, University of Toronto, Toronto, ON, CA
123. Centre for Addiction and Mental Health, Toronto, ON, CA
124. Division of Psychiatry, University College London, London, GB
125. Neuroscience Therapeutic Area, Janssen Research and Development, LLC, Titusville, NJ, US
126. Institute of Molecular and Cell Biology, University of Tartu, Tartu, EE
127. Psychosis Research Unit, Aarhus University Hospital, Risskov, Aarhus, DK
128. University of Liverpool, Liverpool, GB
129. Mental Health Center Copenhagen, Copenhagen Universtity Hospital, Copenhagen, DK
130. Human Genetics and Computational Biomedicine, Pfizer Global Research and Development, Groton, CT, US
131. Psychiatry, Harvard Medical School, Boston, MA, US
132. Psychiatry, University of Iowa, Iowa City, IA, US
133. Department of Psychiatry and Behavioral Sciences, Johns Hopkins University, Baltimore, MD, US
134. Department of Psychiatry and Psychotherapy, University Medical Center Göttingen, Goettingen, Niedersachsen, DE
135. Human Genetics Branch, NIMH Division of Intramural Research Programs, Bethesda, MD, US
136. Faculty of Medicine, University of Iceland, Reykjavik, IS
137. Child and Adolescent Psychiatry, Erasmus MC, Rotterdam, Zuid-Holland, NL
138. Psychiatry, Erasmus MC, Rotterdam, Zuid-Holland, NL
139. Psychiatry, Dalhousie University, Halifax, NS, CA
140. Division of Epidemiology, New York State Psychiatric Institute, New York, NY, US
141. Department of Clinical Medicine, University of Copenhagen, Copenhagen, DK
142. Department of Medical & Molecular Genetics, King's College London, London, GB
143. Psychiatry & Behavioral Sciences, Stanford University, Stanford, CA, US

144. NIHR BRC for Mental Health, King's College London, London, GB
145. Genetics, University of North Carolina at Chapel Hill, Chapel Hill, NC, US
146. Psychiatry, University of North Carolina at Chapel Hill, Chapel Hill, NC, US

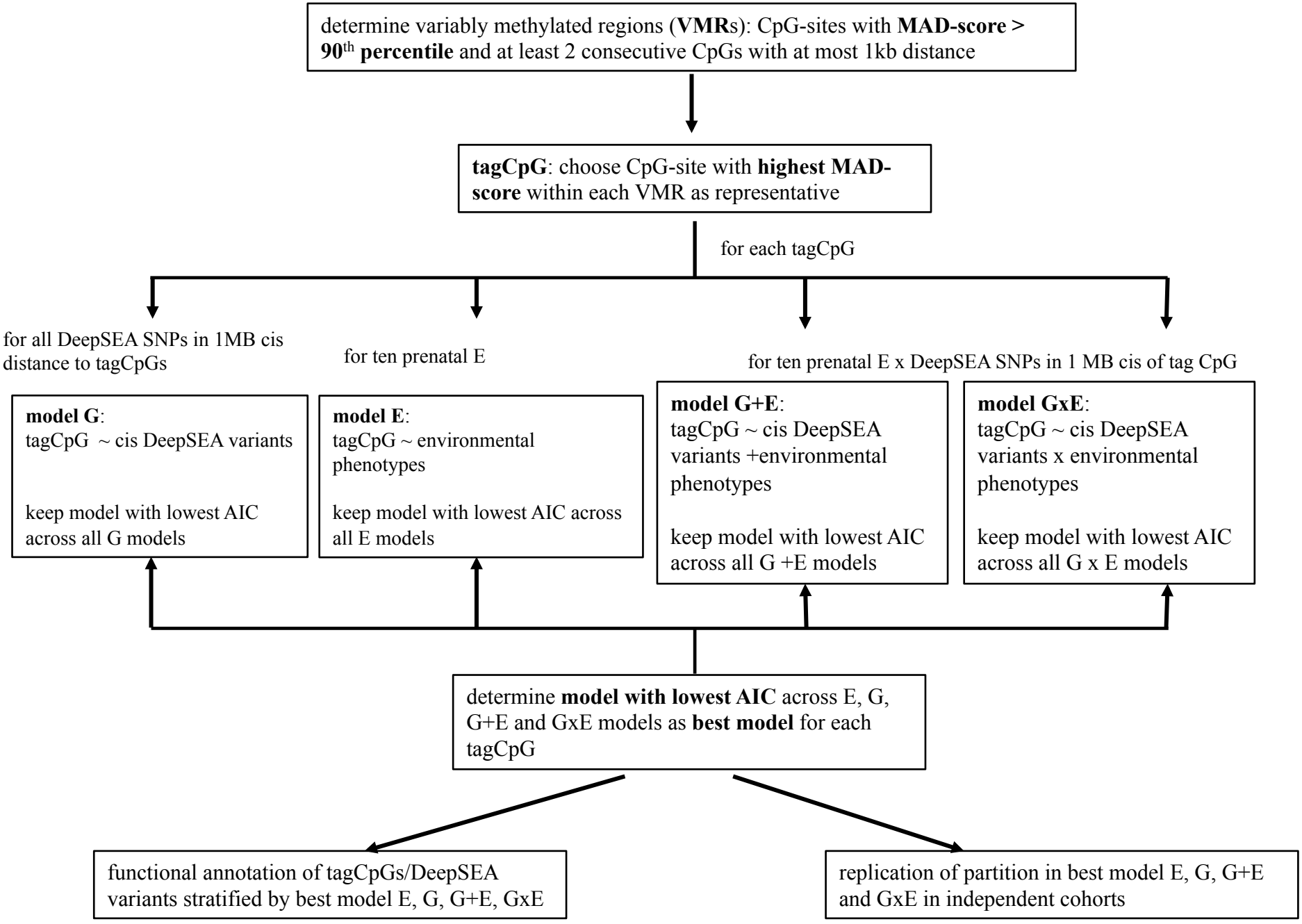
determine variably methylated regions (**VMR**s): CpG-sites with **MAD-score > 90th percentile** and at least 2 consecutive CpGs with at most 1kb distance
tagCpG: choose CpG-site with **highest MAD-score** within each VMR as representative
for each tagCpG
for all DeepSEA SNPs in 1MB cis distance to tagCpGs
for ten prenatal E
for ten prenatal E x DeepSEA SNPs in 1 MB cis of tag CpG
model G: tagCpG ~ cis DeepSEA variants
keep model with lowest AIC across all G models
model E: tagCpG ~ environmental phenotypes
keep model with lowest AIC across all E models
model G+E: tagCpG ~ cis DeepSEA variants +environmental phenotypes
keep model with lowest AIC across all G +E models
model GxE: tagCpG ~ cis DeepSEA variants x environmental phenotypes
keep model with lowest AIC across all G x E models
determine **model with lowest AIC** across E, G, G+E and GxE models as **best model** for each tagCpG
functional annotation of tagCpGs/DeepSEA variants stratified by best model E, G, G+E, GxE
replication of partition in best model E, G, G+E and GxE in independent cohorts

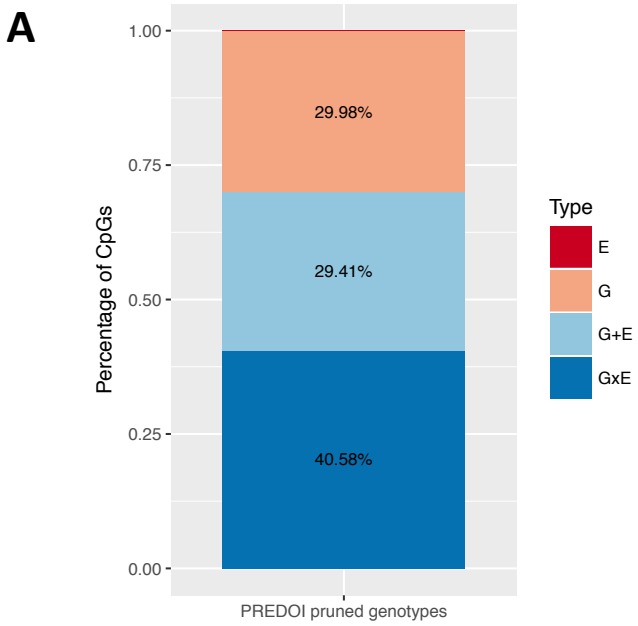
A
1.00
0.75
0.50
0.25
0.00
Percentage of CpGs
29.98%
29.41%
40.58%
PREDOI pruned genotypes
Type
E
G
G+E
GxE

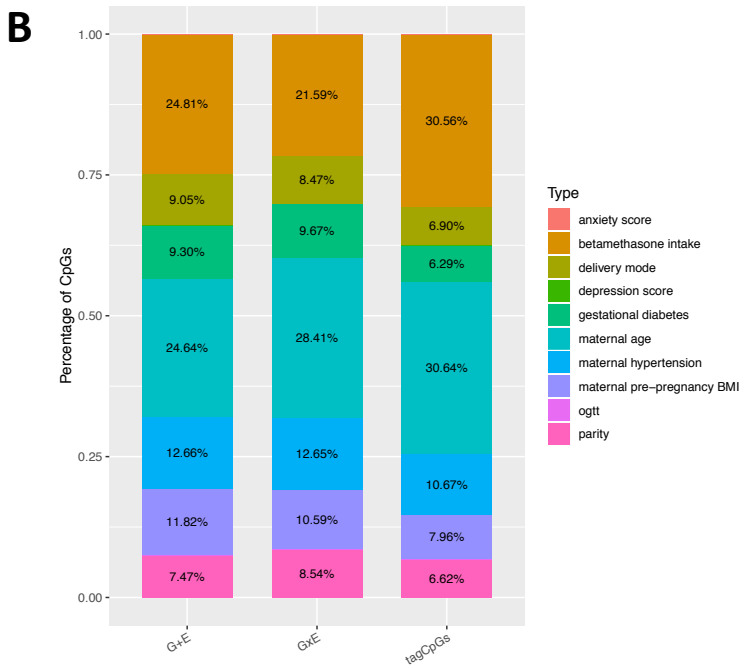
B
1.00
0.75
0.50
0.25
0.00
Percentage of CpGs
24.81%
9.05%
9.30%
24.64%
12.66%
11.82%
7.47%
21.59%
8.47%
9.67%
28.41%
12.65%
10.59%
8.54%
30.56%
6.90%
6.29%
30.64%
10.67%
7.96%
6.62%
G+E
GxE
tagCpGs
Type
anxiety score
betamethasone intake
delivery mode
depression score
gestational diabetes
maternal age
maternal hypertension
maternal pre−pregnancy BMI
ogtt
parity

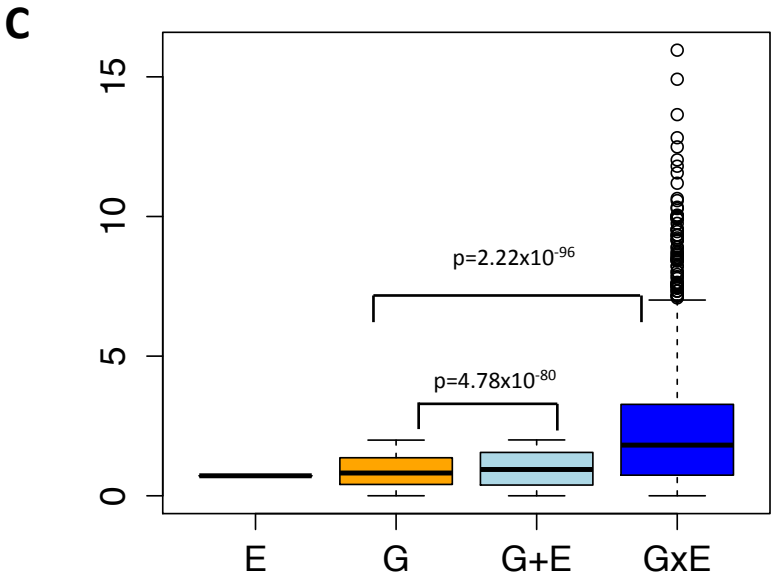
C
0
5
10
15
p=2.22x10-96
p=4.78x10-80
E
G
G+E
GxE

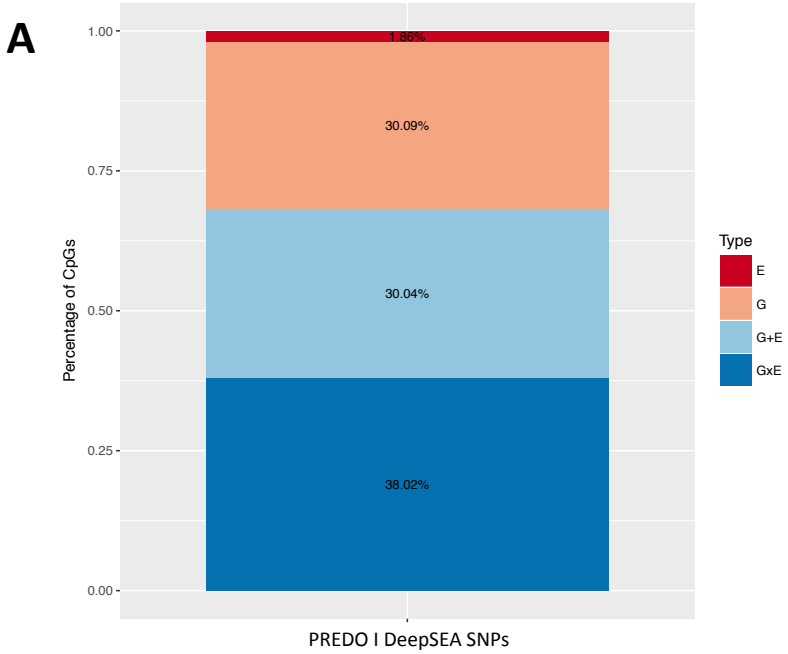
A
1.00
0.75
0.50
0.25
0.00
Percentage of CpGs
1.86%
30.09%
30.04%
38.02%
PREDO I DeepSEA SNPs
Type
E
G
G+E
GxE

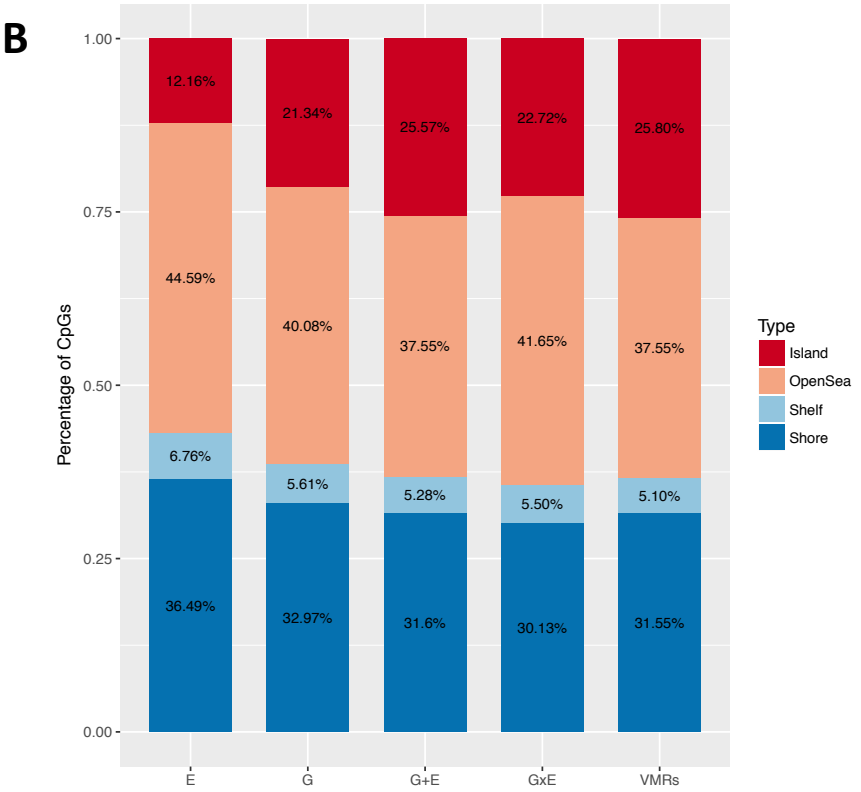
B
1.00
0.75
0.50
0.25
0.00
Percentage of CpGs
12.16%
44.59%
6.76%
36.49%
21.34%
40.08%
5.61%
32.97%
25.57%
37.55%
5.28%
31.6%
22.72%
41.65%
5.50%
30.13%
25.80%
37.55%
5.10%
31.55%
E
G
G+E
GxE
VMRs
Type
Island
OpenSea
Shelf
Shore

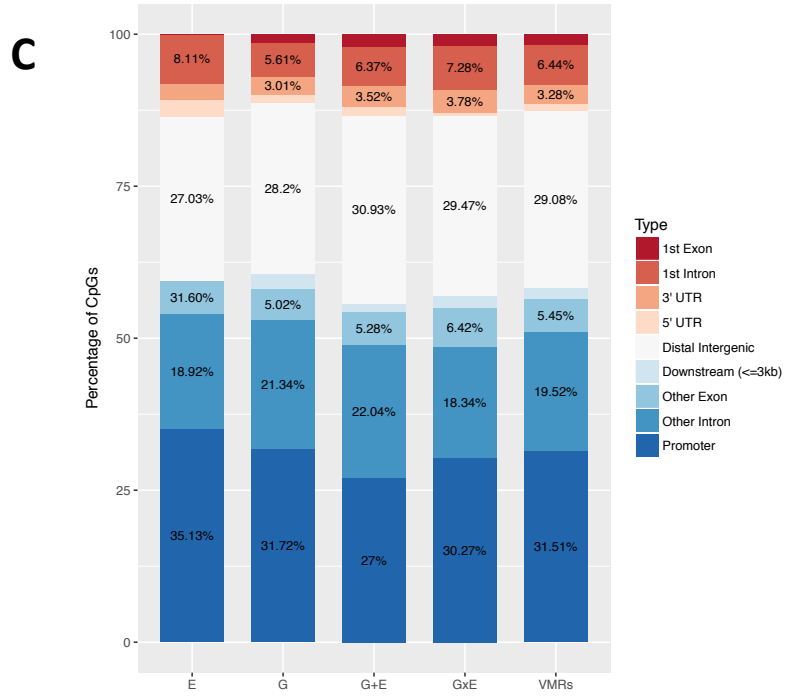
C
100
75
50
25
0
Percentage of CpGs
8.11%
27.03%
31.60%
18.92%
35.13%
5.61%
3.01%
28.2%
5.02%
21.34%
31.72%
6.37%
3.52%
30.93%
5.28%
22.04%
27%
7.28%
3.78%
29.47%
6.42%
18.34%
30.27%
6.44%
3.28%
29.08%
5.45%
19.52%
31.51%
E
G
G+E
GxE
VMRs
Type
1st Exon
1st Intron
3' UTR
5' UTR
Distal Intergenic
Downstream (<=3kb)
Other Exon
Other Intron
Promoter

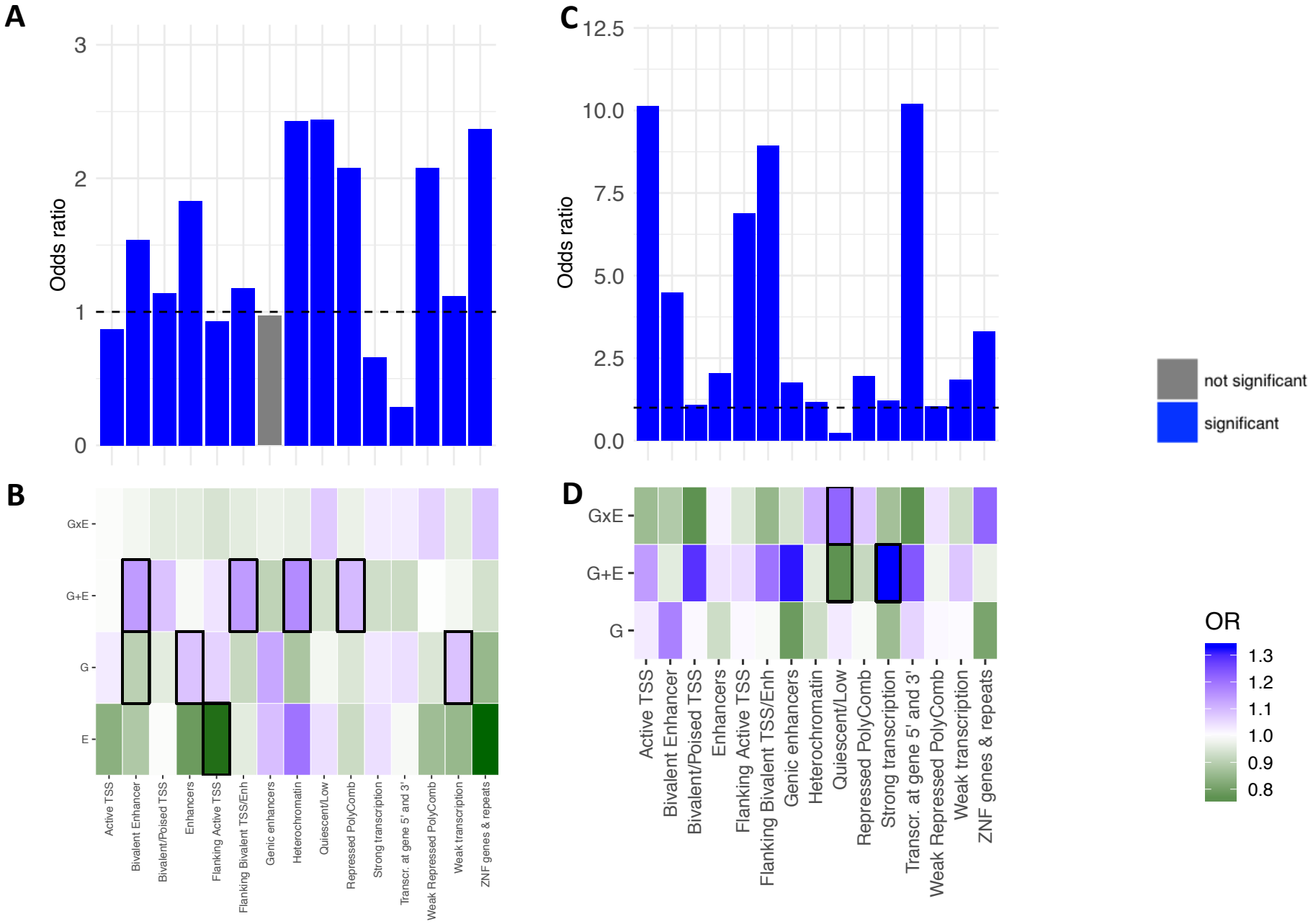
A
Odds ratio
3
2
1
0
C
Odds ratio
12.5
10.0
7.5
5.0
2.5
0.0
not significant
significant
B
GxE
G+E
G
E
Active TSS
Bivalent Enhancer
Bivalent/Poised TSS
Enhancers
Flanking Active TSS
Flanking Bivalent TSS/Enh
Genic enhancers
Heterochromatin
Quiescent/Low
Repressed PolyComb
Strong transcription
Transcr. at gene 5' and 3'
Weak Repressed PolyComb
Weak transcription
ZNF genes & repeats
D
GxE
G+E
G
Active TSS
Bivalent Enhancer
Bivalent/Poised TSS
Enhancers
Flanking Active TSS
Flanking Bivalent TSS/Enh
Genic enhancers
Heterochromatin
Quiescent/Low
Repressed PolyComb
Strong transcription
Transcr. at gene 5' and 3'
Weak Repressed PolyComb
Weak transcription
ZNF genes & repeats
OR
1.3
1.2
1.1
1.0
0.9
0.8

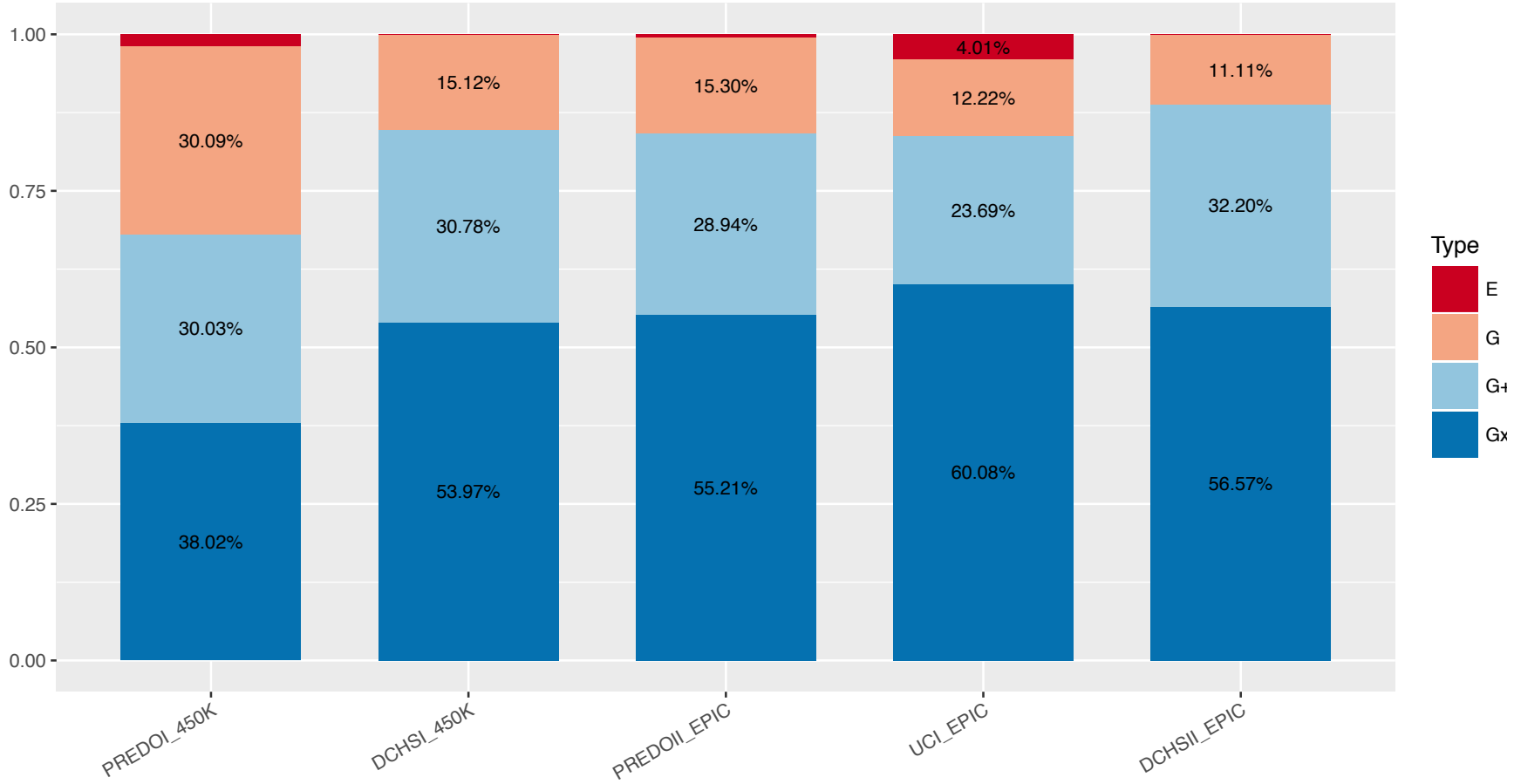
1.00
0.75
0.50
0.25
0.00
30.09%
30.03%
38.02%
15.12%
30.78%
53.97%
15.30%
28.94%
55.21%
4.01%
12.22%
23.69%
60.08%
11.11%
32.20%
56.57%
PREDOI_450K
DCHSI_450K
PREDOII_EPIC
UCI_EPIC
DCHSII_EPIC
Type
E
G
G+
Gx

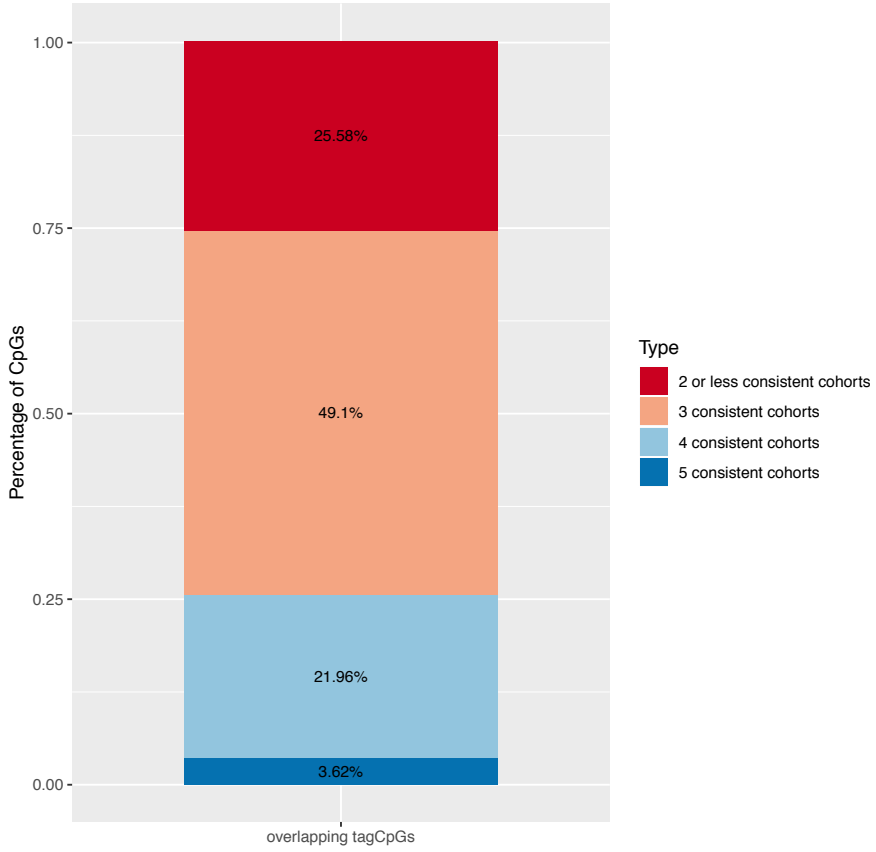
1.00
0.75
0.50
0.25
0.00
Percentage of CpGs
25.58%
49.1%
21.96%
3.62%
overlapping tagCpGs
Type
2 or less consistent cohorts
3 consistent cohorts
4 consistent cohorts
5 consistent cohorts

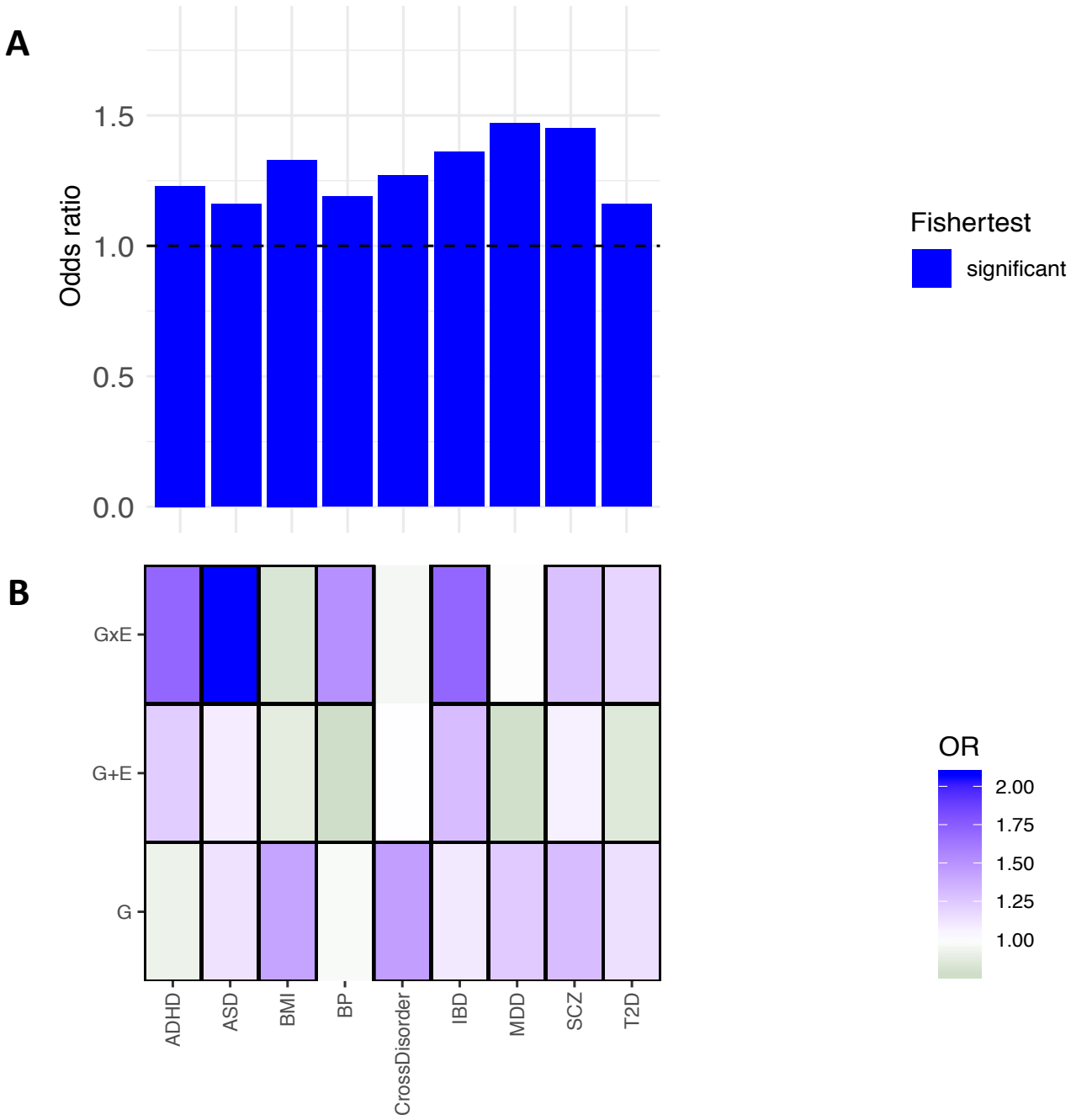
A
1.5
1.0
0.5
0.0
Odds ratio
Fishertest
significant
B
GxE
G+E
G
ADHD
ASD
BMI
BP
CrossDisorder
IBD
MDD
SCZ
T2D
OR
2.00
1.75
1.50
1.25
1.00